Airbursts and Cratering Impacts

2024 | Volume 2 | Pages: 1–33 | e-location ID: e20240001
DOI: 10.14293/ACI.2024.0001

Research Article

The Hopewell Cosmic Airburst Event: A review of the empirical evidence

Kenneth Barnett Tankersley[1,*], Stephen D. Meyers[2,a] and Stephanie A. Meyers[3]

[1]Department of Anthropology, University of Cincinnati, Cincinnati, OH 45221, USA; [2]Department of Geology, University of Cincinnati, Cincinnati, OH 45221, USA; [3]Department of Biology, University of Cincinnati, Cincinnati, OH 45221, USA

[a]Alumnus.
*Correspondence to: Kenneth Barnett Tankersley, E-mail: tankerkh@uc.edu

Received: 11 January 2024; Revised: 11 January 2024; Accepted: 12 January 2024; Published online: 3 February 2024

How to cite: Tankersley K.B., et al. The Hopewell Cosmic Airburst Event: A review of the empirical evidence. *Airbursts and Cratering Impacts*. 2024 | Volume 2 | Issue 1 | Pages: 1–33 | DOI: 10.14293/ACI.2024.0001

ABSTRACT

Abundance peaks in microscopic materials, including meltglass, microspherules, Ni, Ir, and Pt have been found in Native American Hopewell-age cultural strata. This discovery includes micrometeorites (possibly pallasites) recovered from heavily burned strata in two Hopewell villages. This evidence suggests that a prehistoric cosmic airburst/impact event occurred in the Ohio River valley. The peaks in these exotic materials only occur within a dark, charcoal-rich burn layer containing a wide range of Hopewell artifacts, and they are not found above or below the layer. Transgenerational oral histories and possibly two unique airburst-shaped Hopewell earthworks at or near the epicenter suggest that Native Americans living in the Ohio River valley may have been eyewitnesses to the impact event. AMS radiocarbon ages (n = 15) obtained directly from cultural and geological contexts indicate that the airburst/impact event occurred within a 70-year window from 1640-1570 cal BP. The Hopewell culture existed from ~2100-1500 cal BP and suffered a severe decline beginning ~1650 cal BP, suggesting that the proposed impact event occurred near the end of that span. After the proposed event, the hallmarks of the Hopewell culture, such as monumental landscape architecture, the largest geometric earthen enclosures in the world, intricate hilltop water management systems, massive burial mounds, and extensive ceremonial centers, were no longer constructed in the area impacted by the airburst. We propose that this cosmic airburst/impact event catalyzed the economic and sociopolitical decline and reorganization of the Hopewell cultural complex in the Ohio River valley for villages directly affected by the proposed airburst.

KEYWORDS

impact event, micrometeorites, meltglass, microspherules, platinum, iridium, stable carbon isotopes, ethnoastronomy, archaeoastronomy, Tunguska

Introduction

For more than 250 years, scientists have written about the effects of cosmic impact events on economic, political, and social systems [1–5], whether from single impactors or multiple airbursts/impacts by fragments of a giant comet [1, 6–8]. As early as 1755, Thomas Wright expressed concern that a cosmic impact event could lead to cultural decline [1]. In 1806, Marquis de Laplace warned that an impact event would have dramatic human consequences [1]. Their concerns about potential cultural responses to an impact event were based on astronomical data and observations. Like the Moon, the Earth has experienced relatively constant cosmic

impacts over the past three billion years [1, 9], but unlike the Moon, evidence of these cosmic events on Earth has been obscured by the geological processes of erosion and weathering.

Earth-impacting asteroids, comets, and their fragments can result in cratering, ejecta deposition, overpressure shock, seismic shaking, tsunamis, thermal radiation, and wind blasts [9]. Modern disaster managers recognize that these side effects could be devastating, if not catastrophic, to human life. The cosmic impact events that occur on or over land are the most disastrous to human populations and their cultures [9]. The long-term environmental effects of medium to large ocean impactors can be even more destructive [10]. In comparison, airburst events by small oceanic-impacting cosmic objects are relatively benign to human populations but can be devastating over land [11]. Consequently, NASA has funded the Asteroid Terrestrial-impact Last Alert System (ATLAS), an automated system of eight telescopes, which can provide a one-week warning for a > 45 m diameter asteroid or comet and a three-week warning for an asteroid or comet > 120 m in diameter [12].

Numerous cosmic impact events have occurred on the Earth over the last 4.5 billion years, including some with catastrophic consequences for past humans and their cultures [13, 14]. On Sunday, April 15, 2018, a 48-110 m wide asteroid (2018 GE3) came within 192,000 km of the Earth (half the distance to the Moon). It was more than three times the size of the asteroid that caused the 1908 Tunguska airburst [15]. Because of these dangers, it is crucial to research past occurrences and future possibilities of such catastrophic events.

The Hopewell culture

The term "Hopewell" refers to an archaeological cultural complex of the Middle Woodland cultural period in the Midwestern United States from ~2100 to 1500 calendar years before present or cal BP (~100 BCE to 500 CE). The archaeological record of Hopewell includes ancestral Algonquian and Iroquoian burial grounds, habitations, intricate water management systems, and monumental landscape architecture [16, 17]. Their descendants include members of the Adawe, Anishinaabe, Haudenosaunee, Lenape, Myaamiaki, Piqua, Shawano, and Wyandotte (Tionontati, Attignawantan, and Wenrohronon) tribes [18].

Archaeological interpretations of Hopewell culture and all previously published literature on meteorites excavated from Hopewell archaeological sites have been written by settler colonists [16–18], and typically, Indigenous cultural accounts have been minimized or ignored. Even the archaeological term "Hopewell" was named after a settler colonist, Mordecai Cloud Hopewell [16–18]. For some 200 years, the term Hopewell was ethnocentrically misconstrued by many as an ancient "lost white race" [17].

More meteorites have been excavated from Hopewell archaeological sites than any other prehistoric cultural period in the Western Hemisphere [19–22]. They occur as unaltered meteorites and as cold-hammered raw materials used to manufacture cultural materials, such as jewelry and musical instruments [19, 20]. For more than 100 years, the anomalously high concentration of Hopewell micrometeorites has been explained in terms of an ancient exchange system or trade network [16–18]. We explore whether some Indigenous stories about meteorites that fell from the sky match the archaeological evidence.

Objective

This study presents evidence from 11 Hopewell archaeological sites to investigate the hypothesis that one or more cosmic airbursts/impacts may have occurred between ~1650 and 1500 cal BP. This objective is based on previous studies identifying a distinctive Hopewell burn layer containing micrometeorites. We also explore criticisms of this hypothesis as presented by Nolan et al. [23].

Results

Searching for potential airburst/impact proxies

Previous investigations of near-surface cosmic airbursts and impacts have used a suite of microscopic impact-related proxies, including micrometeorites, meltglass, microspherules, and positive anomalies of platinum group elements such as iridium (Ir) and platinum (Pt) [5, 11, 24–36]. Consequently, we examined Hopewell sediments from 11 archaeological sites in the Ohio River valley for evidence of these impact-related proxies (Figures 1-16). We also examined the stable carbon isotope values of carbon-rich sediments from a Hopewell-constructed reservoir for evidence of changes in vegetation before, during, and after the proposed airburst event.

Hopewell sediments were identified based on information previously published by others, new radiocarbon ages for this study, chronologically and typologically distinctive artifacts, and earthwork features (Table 1 and Table S1). Supplementary Information can be found at https://zenodo.org/records/10511513 (10.5281/zenodo.10511513). We created Bayesian age-depth models for the three sites with sufficient dating information using OxCal, version 4.4.4, with the IntCal20 calibration curve (Figures 3, 6, and 8). The goal was to test several questions. 1) Are the burn layers Hopewell in age across multiple sites? 2) If so, do the burn layers date to the end of the Hopewell cultural span? 3) Is the suite of ages for the burn layers synchronous within the limits of radiocarbon dating?

Meteoritic material was initially discovered at the Hopewell Turner site by Charles Louis Metz during the late 19th century [19, 37]. No other impact-related proxies have been previously reported at other Hopewell sites, possibly because most of what we know about Hopewell archaeology has come from archaeological excavations conducted more

than 100 years ago, before the widespread use of dry-screening, water-screening, and flotation recovery techniques. Thus, it is not surprising that microscopic evidence of a near-surface cosmic airburst or impact has gone unnoticed during past archaeological investigations.

Archeological site settings

The following figures and captions describe and illustrate the locations and stratigraphy of the sites investigated in this study (Figure 1).

Bayesian tests of potential synchronicity

We conducted two Bayesian tests of synchroneity to explore whether the probability distributions for 17 radiocarbon dates could indicate a contemporaneous event. For details, see Methods below and SI, Methods. First, we used OxCal's Combine routine, which, although it cannot determine whether a group of dates represents a synchronous event, Bayesian analyses can indicate whether dates are statistically diachronous. A chi-squared test is automatically performed with the Combine function,

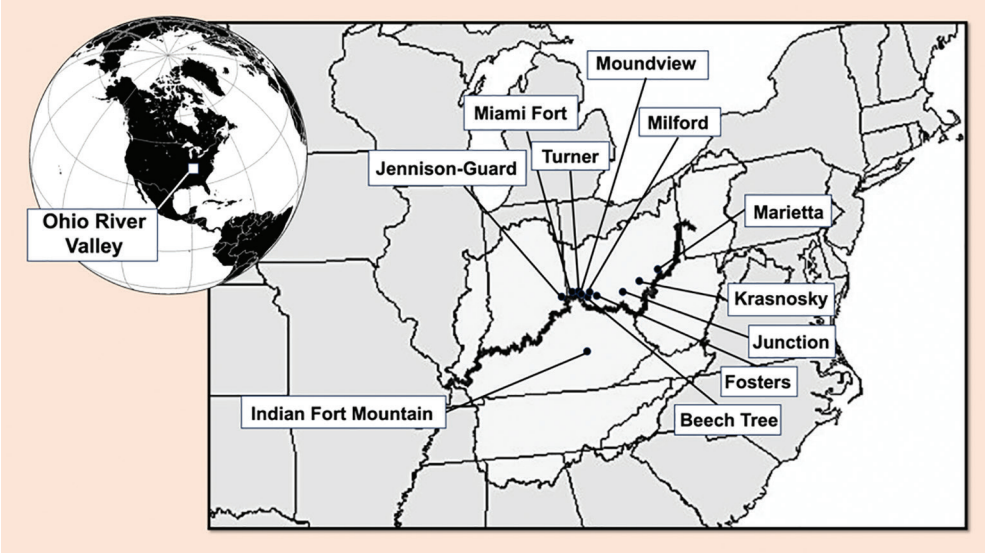

Figure 1: **Hopewell archaeological sites in the Ohio River valley examined for impact-related proxies.**

Table 1: Radiocarbon ages obtained for this study directly from Hopewell impact strata in the Ohio River valley.

Sample	Lab Numbers	^{14}C Age yr BP	Calibrated Age yr BP (Probability)[1]	Depth (m)
Turner village site, Hamilton County, Ohio				
Collagen	Beta-237345	1820 ± 40	1827-1690 (69.9%) 1673-1613 (25.5%)	1.00
Jennison-Guard village site, Unit A, Dearborn County, Indiana				
Collagen	Beta-547669	1630 ± 30	1568-1409 (95.4%)	0.55-0.85
Collagen	Beta-547668	1680 ± 30	1695-1665 (13.8%) 1625-1518 (81.7%)	0.55-0.85
Collagen	Beta-547667	1740 ± 30	1705-1549 (95.4%)	0.55-0.85
Jennison-Guard paleo-swale, Unit B, Dearborn County, Indiana				
Wood Charcoal	Beta-547670	1730 ± 30	1703-1652 (32.6%) 1645-1544 (62.9%)	1.50
Miami Fort village site, Hamilton County, Ohio[2]				
Wood Charcoal	M-1869	1680 ± 130	1867-1855 (1%) 1835-1310 (95%)	0.91-1.59

Other Hopewell radiocarbon dates on burn layers by other researchers are reported in Supplementary Information, Table S1. Supplementary Information can be found at https://zenodo.org/records/10511513 (10.5281/zenodo.10511513).
[1]Oxcal Calibration Program 4.4.
[2]Crane H. R., Griffin, J. B., (1968). University of Michigan Radiocarbon Dates **10**, 61-114.

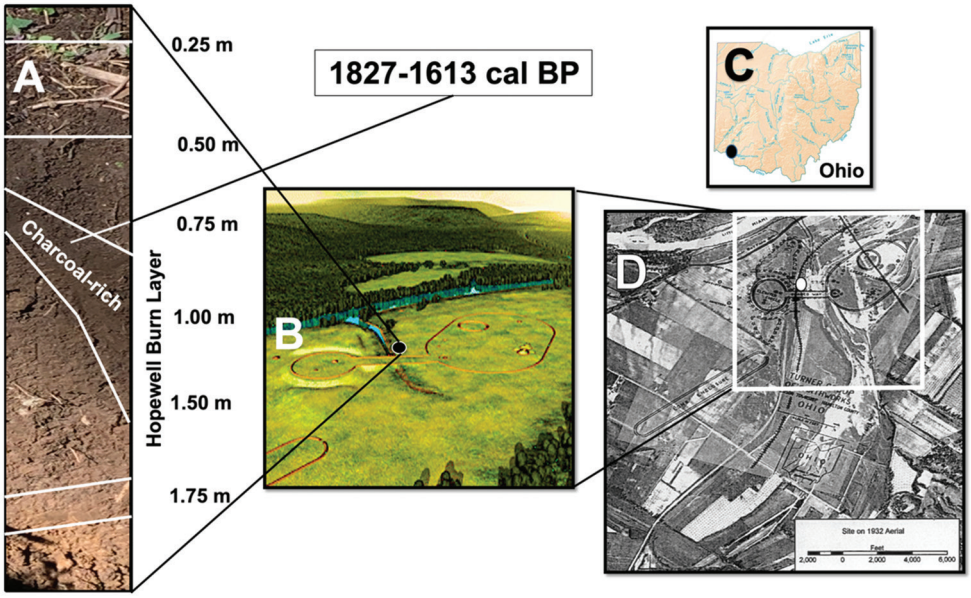

Figure 2: Geographic and stratigraphic location of the Turner site. (A) Stratigraphic profile illustrating the location of the charcoal-rich Hopewell burn layer and associated calibrated AMS radiocarbon age. Note the inclination and highly variable depths of the burn layer. The burn layer contains abundance peaks in micrometeorites, microspherules, Ni, Pt, and Ir. **(B)** Center for the Electronic Reconstruction of Historical and Archaeological Sites (CERHAS) reconstruction of the Turner site earthworks and location of the area sampled. **(C)** Location of the Turner site in southwestern Ohio. **(D)** Overlay of the 1887 Hosbrook and 1960 Starr maps of the Turner site projected onto a georeferenced 1932 aerial photo. See also Tables S2, S3, S4.

and an error message is generated if the confidence limits drop below 5%. Although one Jennison-Guard date was rejected as too young, for 16 of the 17 dates on the Hopewell burn layers, OxCal determined that they passed the chi-squared test and can be combined. In other words, they could be statistically synchronous within the limits of radiocarbon dating and Bayesian analysis (Figure 17, Table S11). This finding is contrary to the claims by Nolan et al. [23] who claim a chi-squared test failed to support a single event.

Second, we used OxCal's Sequence and Difference codes to determine the most likely common age interval for the 17 radiocarbon dates on the Hopewell burn layer. In this test, if the computed interval at 95% CI allows for a total overlap, i.e., includes zero years (often presented as "-5"), then synchroneity is possible. On the other hand, if the estimated interval at 95% CI includes only non-zero values, then it is probable that the calibrated dates are too different, and synchroneity can be rejected. OxCal rejected three of the 17 younger and older dates, but for 14 of 17, the program computed a minimum interval of zero years (displayed as "-5") at 68.3%, 95.4%, and 99.7% CI. Thus, synchronicity for the Hopewell burn layer at four sites is statistically possible and cannot be rejected (Figure 18, Table S12).

Using the results from the Difference command in the Sequence code, we calculated the modeled age span of the Hopewell burn layer by using the values for median age and uncertainty from the Start and End boundaries. The range is 70 ± 60 years or 1640-1570 cal BP, which most likely includes the proposed impact event that could be synchronous across the four sites.

Meteoritic material

Meteoritic material was initially discovered at the Turner site by Charles Louis Metz during the late 19th century [19, 37]. Approximately 1,600 g of pallasites were collected from what Metz labeled "altars" in Mound 3 and Mound 4 [19–21]. AMS radiocarbon ages from botanical remains collected from Mound 3 range between 1805 and 1404 cal BP (Table S1). At the time of Metz's excavations, the Turner site consisted of a complex of Hopewell geometric earthworks, mounds, and a village covering more than 165 ha in Hamilton County, Ohio [19, 37, 38].

After more than a century of sand and gravel mining, only ~1% of the site remains: ~0.05 ha of the northern-most margin of the village and ~0.13 ha containing a segment of the southern-most earthwork (Figure 2). Sediment samples were collected from a 1 m^2 test unit in village portion of the site from which the calibrated radiocarbon age of 1827-1613 cal BP was obtained (Table 1, Table S1). A neodymium magnet was used to look for micrometeorites in samples collected from the exposed strata. We recovered 14 granular, fine gravel-to-coarse-sand-sized iron and stony-iron melted material from ~25 kg of sediment obtained from the charcoal-rich Hopewell burn layer (i.e., less than 1/kg)

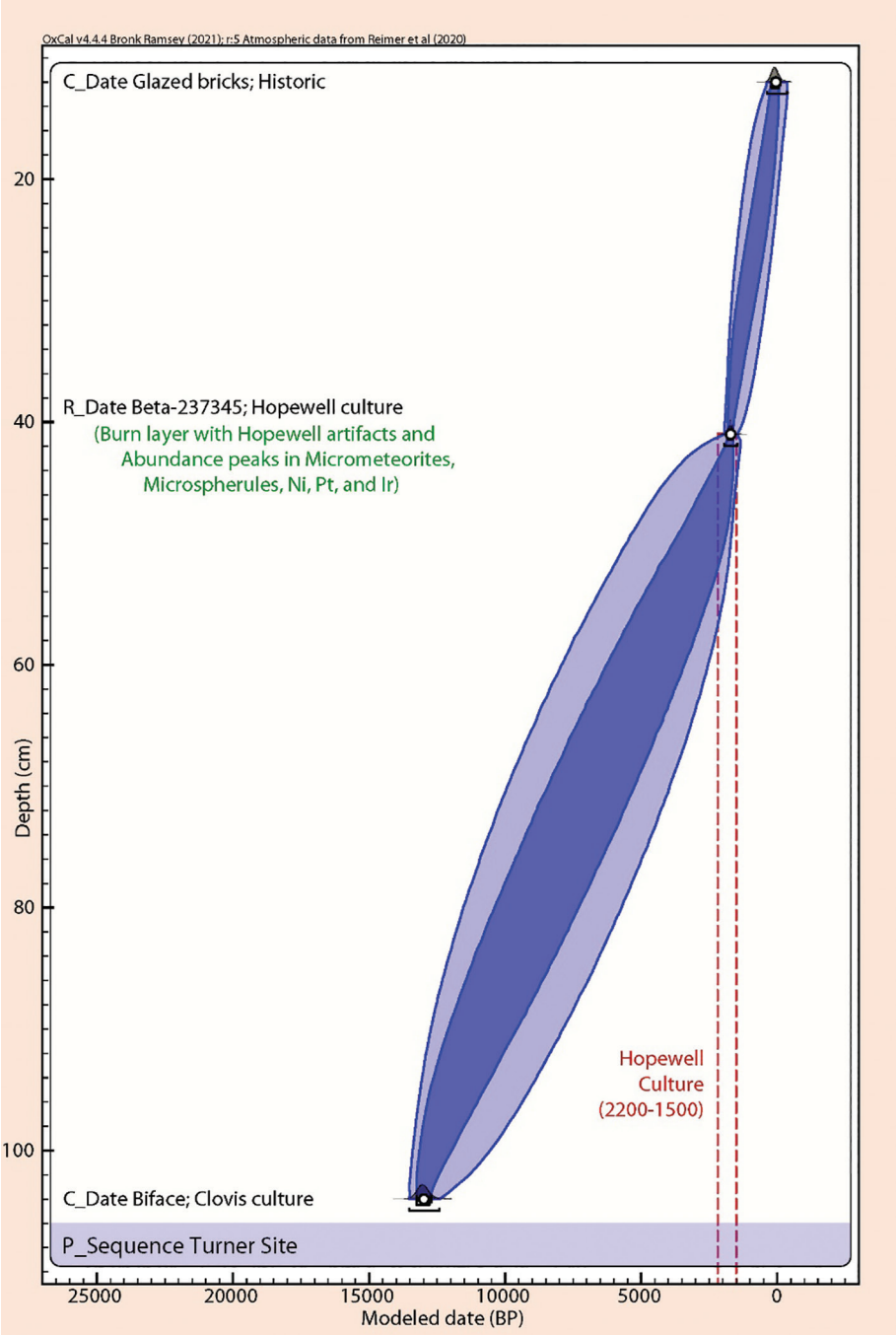

Figure 3: Bayesian age-depth model for the Turner site. Bayesian analysis indicates the burn layer dates to ~1715 ± 105 (1940-1470 cal BP at 95.4% Confidence Interval (CI)). The results show that the age overlaps the end of the Hopewell cultural span (red dashed line: 2100-1500 cal BP). The layer contains Hopewell artifacts co-occurring with peak concentrations of micrometeorites, microspherules, Ni, Pt, and Ir with few to none above or below, including in the layers containing Clovis cultural artifacts, for which typical cultural age spans were used. For the Bayesian code and tables, see Table S5.

(Figure 19). They matched the geochemistry of pallasites, were recovered from heat-altered, clay-lined, rectangular basin-shaped features built on top of a ~25 cm heavily burned stratum (see Supplementary Information for more details). Micrometeorites were absent above and below the burn layer.

Weathered Widmanstätten crystal patterns (i.e., Thomson structures) distinctive of octahedrite and pallasites were found on the surface of a micrometeorite from the Turner site (Figure 20, Table S3). The surface morphology of the Turner site fine gravel-to-sand size specimens is distinctive of individual micrometeorites and not the debris from the ancient

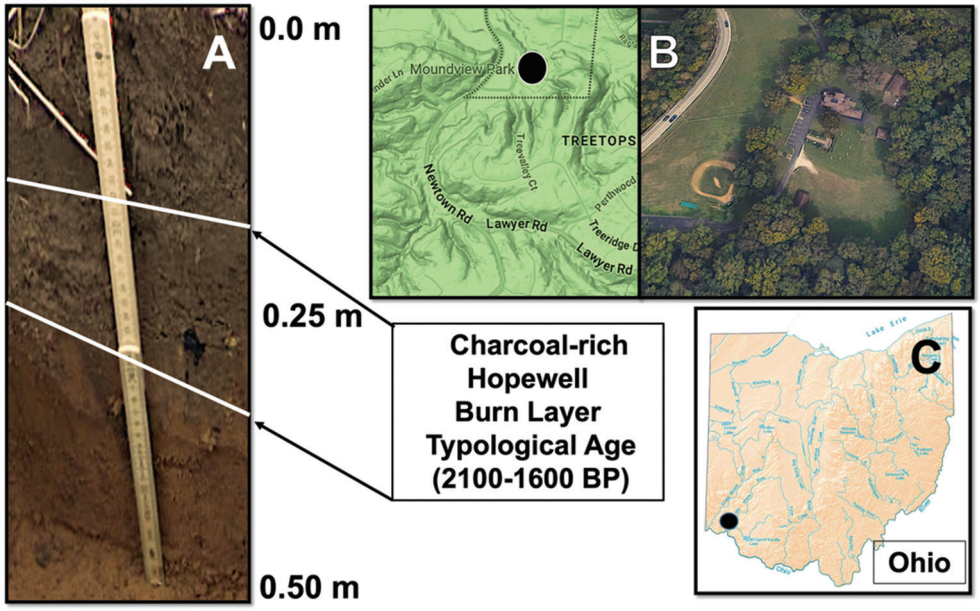

Figure 4: **Geographic and stratigraphic location of the Moundview site. (A)** Stratigraphic profile illustrating the location of the charcoal-rich Hopewell burn layer and typological age. Note the inclination and highly variable depths of the burn layer. The burn layer contains abundance peaks in microspherules, Pt, and Ir. **(B)** Location of the Moundview site along McCollough Run, a tributary of the Little Miami River valley. **(C)** The location of the Moundview site in southwestern Ohio. See also Table S2, S6.

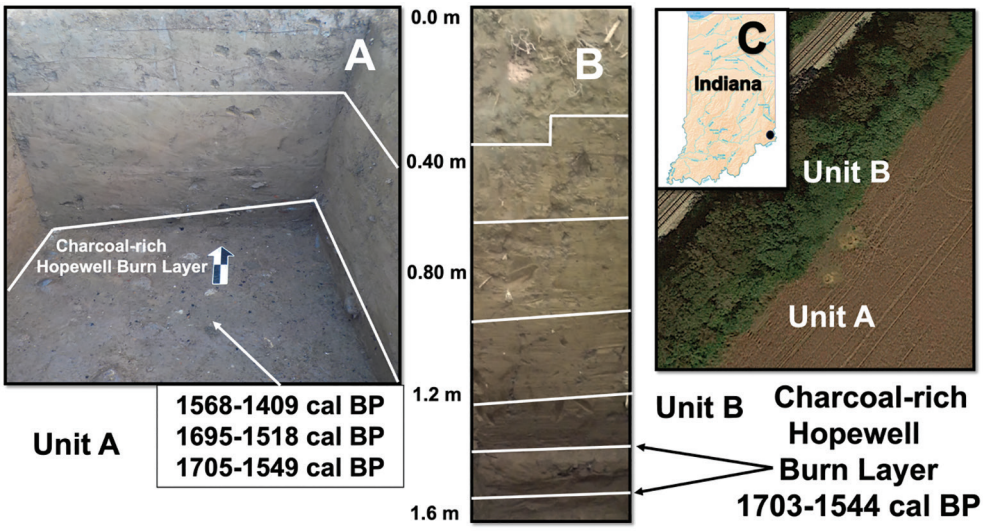

Figure 5: **Geographic and stratigraphic location of the Jennison-Guard site. (A)** Stratigraphic profile of Unit A illustrating the location of the charcoal-rich Hopewell burn layer and calibrated radiocarbon ages. Note the variable depths of the burn layer, the only one observed in the occupational history. **(B)** Stratigraphic profile of Unit B illustrating the location of the charcoal-rich Hopewell burn layer and calibrated radiocarbon age. The burn layer contains abundance peaks in microspherules, Pt, and Ir. **(C)** Location of the excavated area (Units A & B) in southeastern Dearborn County, Indiana. See also Table S2, S7.

manufacture of Hopewell material culture. Additionally, the surface morphology of the Turner site specimens differs from micrometeorites described and illustrated from the late Holocene Brenham/Haviland strewnfield in Kiowa County, Kansas and from the Eagle Station strewnfield in Carrol County, Kentucky [35, 36].

Energy-dispersive X-ray spectroscopy (EDS) shows that the microscopic meteorites include NiFe and olivine $(Mg,Fe)_2SiO_4$. (Table 2). EDS also identified phosphorus and aluminum, previously documented in pallasites [39]. Unlike the EDS analysis of a cut, polished, and acid-etched macroscopic pallasite described and illustrated by Nolan et al. [23], the microscopic

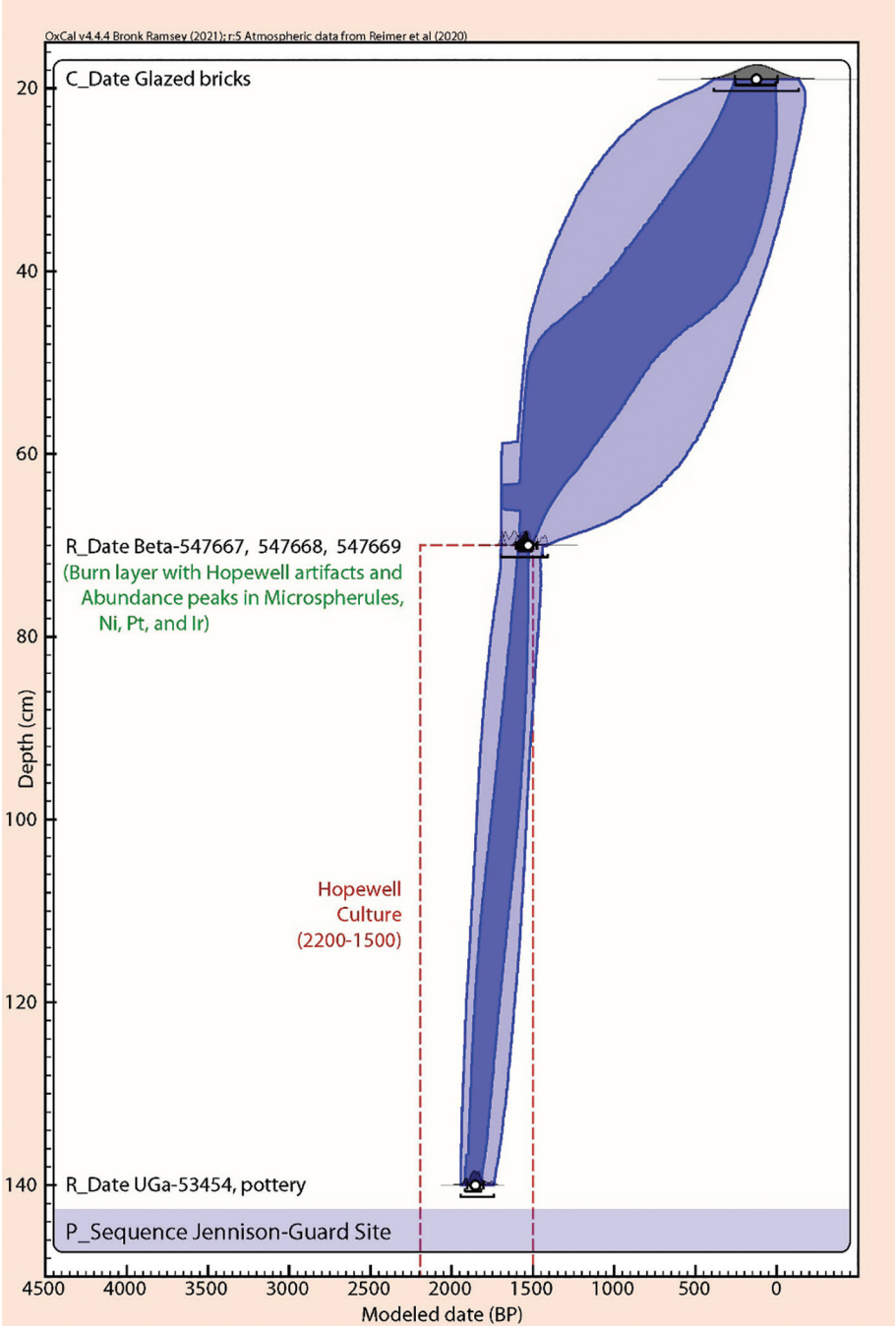

Figure 6: Bayesian age-depth model for the Jennison-Guard site. Bayesian analysis indicates the burn layer dates to ~1530 ± 55 (1700-1405 cal BP at 95.4% Confidence Interval (CI)). The results show that the age overlaps the end of the Hopewell cultural span (red dashed line: 2100-1500 cal BP). The layer contains Hopewell artifacts co-occurring with peak concentrations of microspherules, Pt, and Ir with few to none above or below, including in the layers containing cultural artifacts from the Lake Fort Ancient period and the Adena culture, for which typical cultural age spans were used. For the Bayesian code and tables, see Table S8.

micrometeorites from the Turner site retain elements associated with the clay minerals illite $(K\ H_3O)\cdot(Al,\ Mg,\ Fe)_2\cdot(Si\ Al)_4\cdot O_{10}\cdot[(OH)_2\ (H_2O)]$ and chlorite $(Mg,Fe)_3\ (Si,Al)_4\ O_{10}\ (OH)_2\cdot(Mg,Fe)_3(OH)$, which occur in the soils of the Turner site [37]. Clay minerals have a high adhesive strength, and microscopic particles remain after washing with water.

Meltglass

Petrographic thin sections were made of the micrometeorite-bearing Hopewell sediments of the Turner site. Vesicular, scoria-like meltglass was found in the thin sections co-occurring with microspherules and carbonized plant remains (Figure 21). Near-surface cosmic airbursts

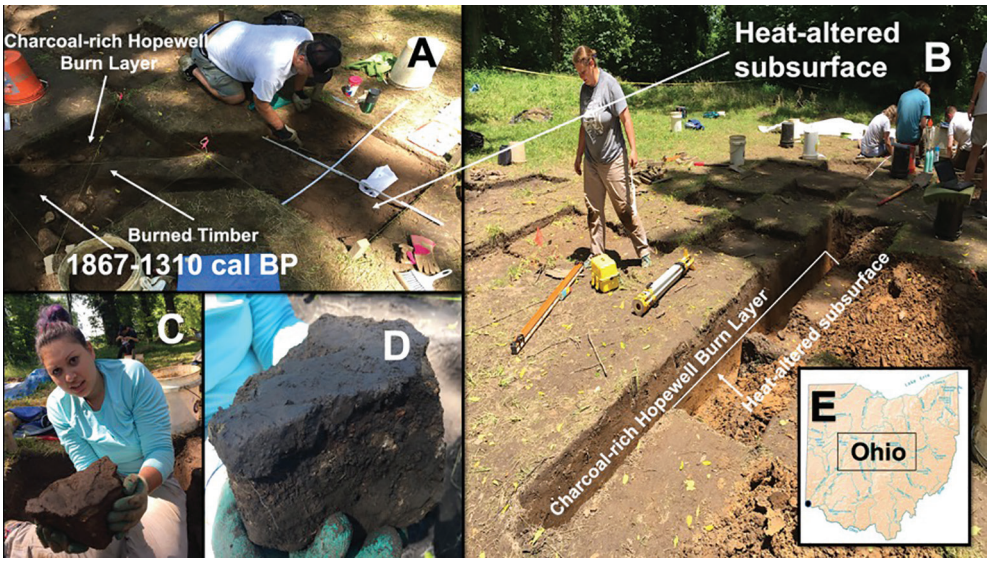

Figure 7: Geographic and stratigraphic location of the Miami Fort site. (A) Excavation of the charcoal-rich Hopewell burn layer, heat-altered subsurface, and calibrated radiocarbon age. **(B)** Stratigraphic trench profile exposing the charcoal-rich Hopewell burn layer and heat-altered subsurface. The burn layer contains abundance peaks in microspherules, Pt, and Ir. **(C & D)** Close-up of the charcoal-rich burn stratum and underlying heat-altered subsurface. **(E)** Location of the Miami Fort site in southwestern Ohio. See also Table S2, S9.

and impacts can form vesicular, scoria-like meltglass [5, 24, 33, 34] that results from the high temperatures and thermo-mechanical shock produced during a cosmic impact event. Meltglass has been found at ground zero at the Trinity nuclear explosion site in New Mexico [40], the Australasian strewnfield in southern China and Australia [40], and Meteor Crater in Arizona [41, 42]. Microscopic meltglass has also been found at the K/T boundary Chicxulub crater in Mexico [43] and multiple sites for the proposed YDB impact event in North America, Europe, and Asia [5, 24, 33].

Microspherules

Magnetic microspherules were recovered from the charcoal-rich Hopewell burn layer in the village portion of the Turner site. The burned surfaces were "peppered" with micrometeorites that are absent in the overlying and underlying strata. Magnetic microspherules include the distinctive dendritic or "Christmas tree" patterns of magnetite crystals, coarse plate-like crystals, polygonal crystal structures, and open vesicles from degassing (Figures 22-24; Table S2) with a melting point of 1,583–1,597°C. Such temperatures are not possible in village campfires but are common in impact events. Distinctive barred olivine textures form during cooling rates between 500 to 2300°C/h (Figure 24) [44]. High-temperature, melt-quenched, and accretionary microspherules are commonly used to indicate extraterrestrial impact events [45–48].

Microspherules result from high-velocity cosmic impact events when Si-rich or Fe-rich minerals melt and condense into microscopic spheroidal particles (Figure 25). They are known as microkrystites if they contain crystallites from the impactor or as microtektites if they are composed of terrestrial materials [45]. They also have been recovered from impact event sites associated with the K/T and Younger Dryas boundaries. Microkrystite microspherules may consist of clinopyroxene, Fe-rich pyroxene, feldspars, olivine, or spinels, and digenetic processes may replace these minerals with clay minerals such as chlorite and glauconite, as well as carbonates, goethite, K-feldspars, quartz, and sericite [45].

Microspherules have been recovered from the Hopewell sediments of all the archaeological sites examined (Figure 1, Figures S2-S11, Table S2). They were exclusively recovered from Hopewell strata and were absent in overlying and underlying strata, suggesting a discrete event rather than a gradual accumulation (Figures 26 and 27). The geographic size distribution of microspherules shows that the estimated direction of the proposed impact was from northeast to southwest (Figure 28).

Platinum group elements

Positive anomalies of platinum group elements such as Ir and Pt have been found in the sediments of previously reported late Holocene age meteor impact sites in Kansas and Kentucky [35, 36]. Since micrometeorites occur at both the Turner and Marietta sites, we should expect to find positive anomalies of platinum group elements at these locations. However, macroscopic and microscopic micrometeorites are absent from the other nine Hopewell sites sampled.

Positive anomalies of the leachate concentrations (ppb) of Ir and Pt were found in the Hopewell sediments of the Turner village site and the nearby Moundview village site 5.5 km away (Table 3). The positive Ir anomalies (1.08 ppb) at these

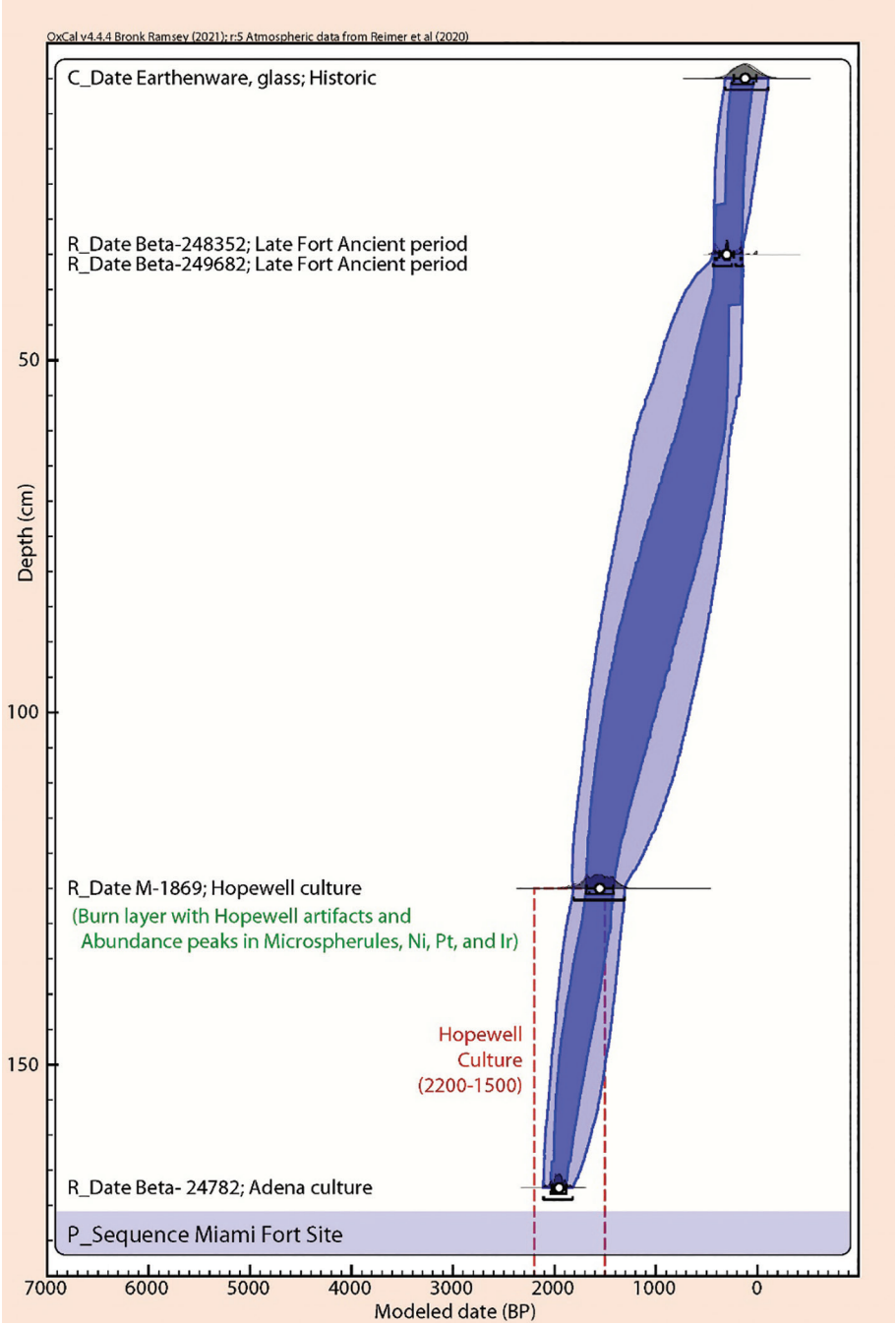

Figure 8: Bayesian age-depth model for the Miami Fort site. Bayesian analysis indicates the burn layer dates to ~1555 ± 130 (1815-1305 cal BP at 95.4% Confidence Interval (CI)). The results show that the age overlaps the end of the Hopewell cultural span (red dashed line: 2100-1500 cal BP). The layer contains Hopewell artifacts co-occurring with peak concentrations of microspherules, Pt, and Ir with few to none above or below, including in the layers containing cultural artifacts from the Late Fort Ancient period, Clovis culture, and the Adena culture, for which typical cultural age spans were used. For the Bayesian code and tables, see Table S10.

sites greatly exceed the natural crustal abundance (0.02 ppb). The Ir leachate concentrations for the Hopewell stratum at the Turner and Moundview villages sites are also within the range of those reported from YD boundary impact event strata (< 0.5 to 3.8 ppb) [3, 49]. The Ir leachate concentrations of the Hopewell strata from all the sites sampled are within the range reported from pallasite bearing impact feature strata in the Brenham/Haviland strewnfield (0.1 to 0.3 ppb) [36].

Positive anomalies of the leachate concentrations of Pt (0.70 to 6.23 ppb) were found in ten of the eleven Hopewell

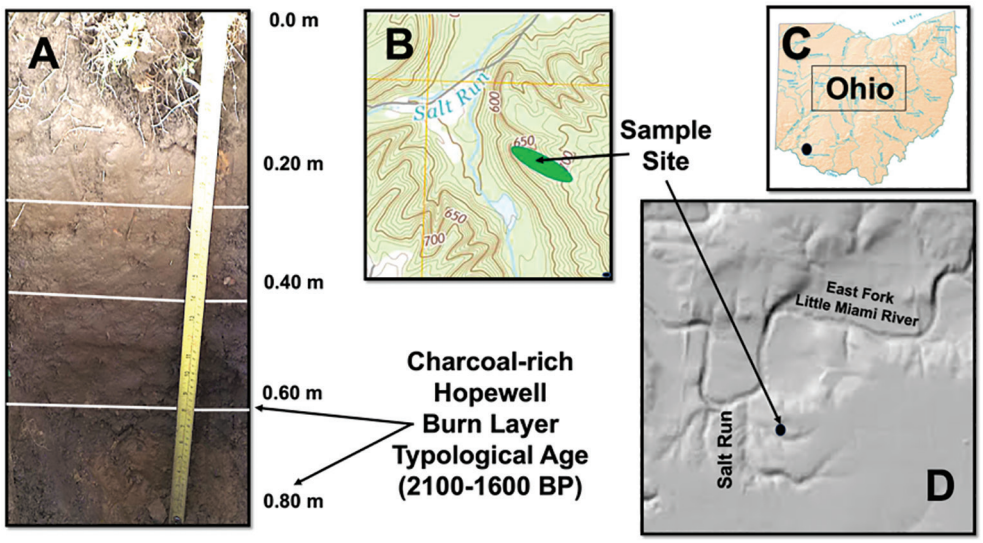

Figure 9: **Geographic and stratigraphic location of the Beech Tree site. (A)** Stratigraphic profile of the charcoal-rich Hopewell burn layer and the underlying heat-altered subsurface. The burn layer contains abundance peaks in microspherules, Pt, and Ir. **(B)** Topographic location of the Beech Tree sample site above Salt Run, a tributary of the East fork of the Little Miami River. **(C)** Location of the Beech Tree site in southwestern Ohio. **(D)** LiDAR image showing the location of the sample site. See also Table S2.

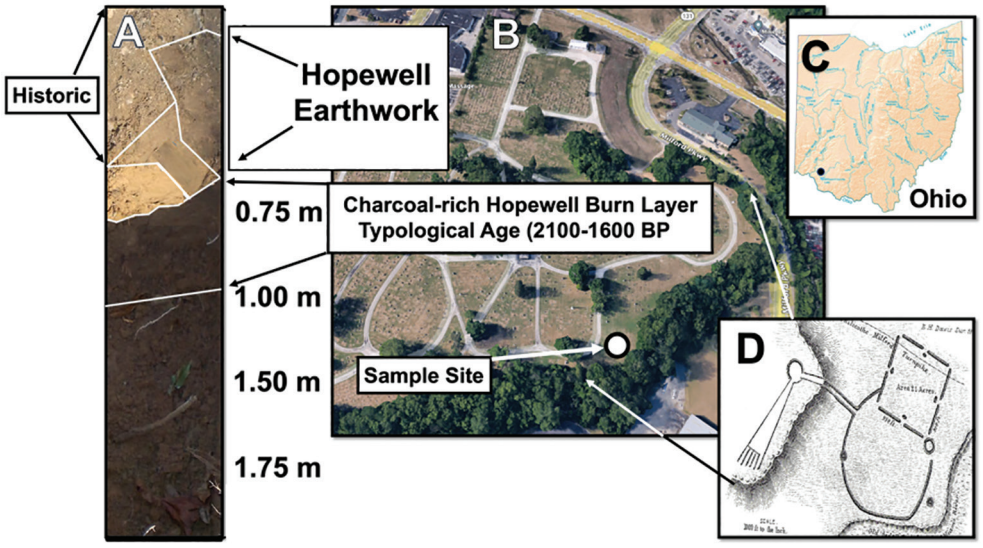

Figure 10: **Geographic and stratigraphic location of the Milford earthworks site. (A)** Stratigraphic profile of the charcoal-rich Hopewell burn layer, typological age, and the juxtaposed overlying historic and anthropogenic Hopewell earthwork sediments (individual loading events outlined). Note the inclination and highly variable depths of the burn layer. The burn layer contains abundance peaks in microspherules, Pt, and Ir. **(B)** Aerial view of the Milford earthworks site. **(C)** Location of the Milford earthworks site in southwestern Ohio. **(D)** The 1847 Ephraim George Squier and Edwin Hamilton Davis map of the Milford earthworks. See also Table S2.

archaeological sites sampled (Table 3, Tables S2, S13-S19). They exceed the natural crustal abundance of Ir (0.5 ppb) and the leachate concentration of Ir reported from pallasite-bearing strata in the meteorite impact features of the Brenham/Haviland strewnfield in Kansas (0.3 to 1.0 ppb) [36]. The Pt level of the Turner village site (6.23 ppb) is well within the ranges reported for the impact event strata at the K-Pg (4.0 to 8.0 ppb) and YD (0.3 to 65.6 ppb) boundaries [3, 49, 50].

Given that the Hopewell stratum of the Turner village site has the highest leachate concentrations of Ir and Pt, it was likely located at or near the epicenter of a near-surface

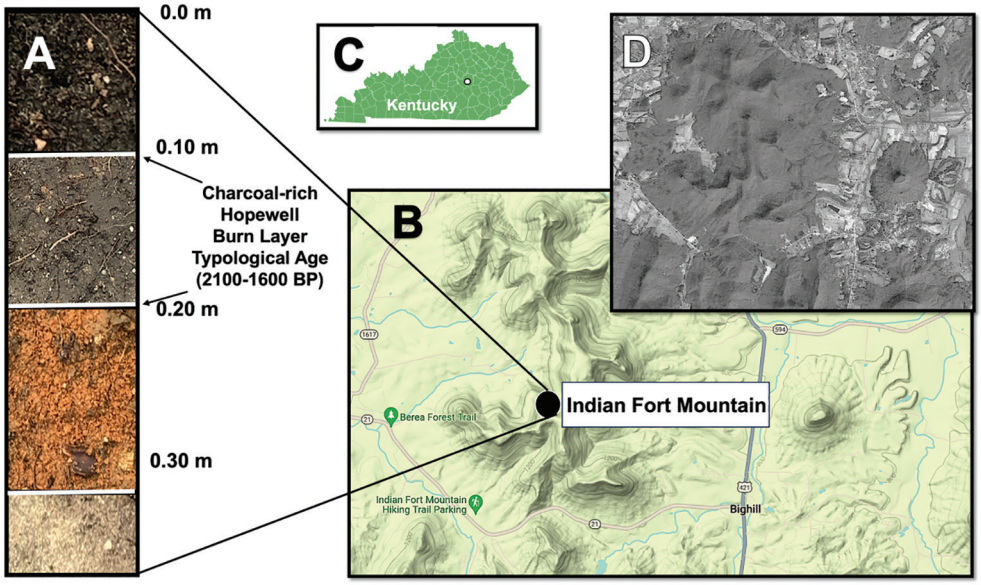

Figure 11: Geographic and stratigraphic location of the Indian Fort Mountain site. (A) Composite stratigraphic profile of the charcoal-rich Hopewell burn layer and typological age. The burn layer contains abundance peaks in microspherules, Pt, and Ir. **(B)** Topographic view of the Indian Fort Mountain sample site. **(C)** Location of the Indian Fort Mountain site in southeastern Kentucky. **(D)** Aerial photo of Indian Fort Mountain. See also Table S2.

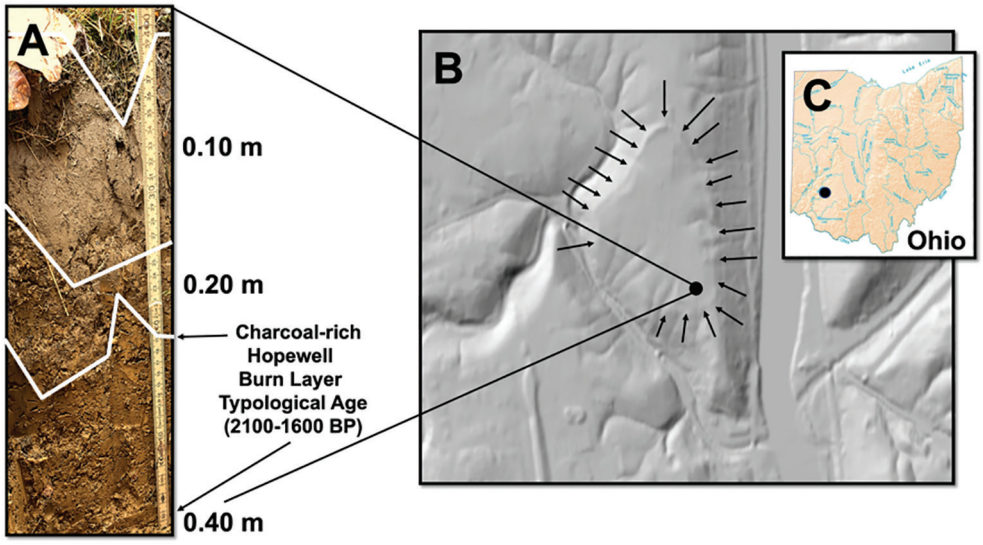

Figure 12: Geographic and stratigraphic location of the Fosters Crossing earthworks site. (A) Stratigraphic profile of the charcoal-rich Hopewell burn layer and typological age. Note the inclination and highly variable depths of the burn layer. The burn layer contains abundance peaks in microspherules, Pt, and Ir. **(B)** LiDAR image of the Fosters earthwork sample site. **(C)** Location of the Fosters earthwork site in southwestern Ohio. See also Table S2.

cosmic airburst or impact event. As with the distribution of microspherules, the leachate concentrations of Ir and Pt in the Hopewell strata from the other archaeological sites sampled in the Ohio River valley decrease with increasing distance from the Turner village site (Table 3, Figures 29-31). Residual plumes of Ir and Pt were reconstructed by plotting the geographic distribution of their leachate concentrations in the strata of the Hopewell archaeological sites sampled (Figures 32 and 33).

Like the microspherules, the residual plumes of Ir and Pt appear in a northeast-to-southwest orientation, which is comparable to the alignment of the airburst-shaped Milford earthwork (Figures 10, 27, 32, 33). The lowest concentrations of the Ir and Pt residual plumes extend in a north-to-south

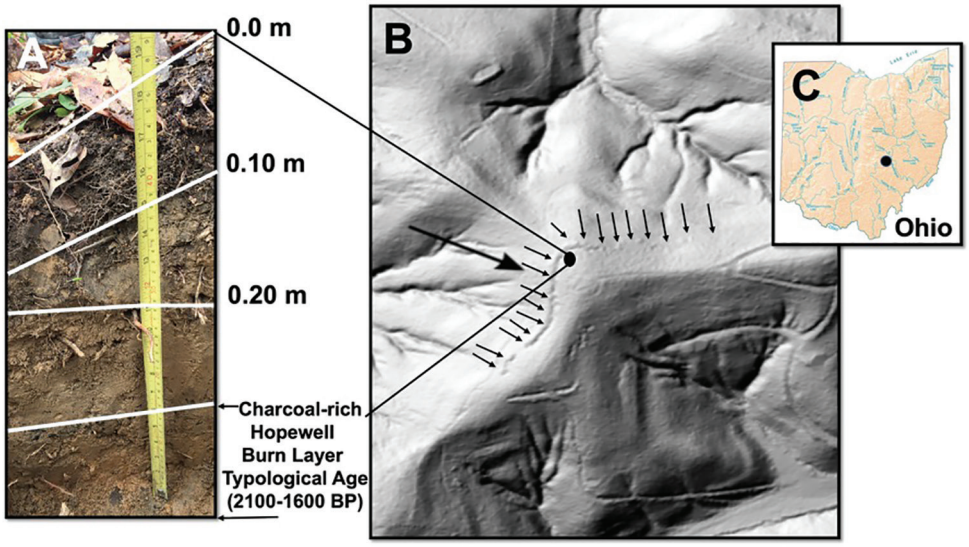

Figure 13: **Geographic and stratigraphic location of the Krasnosky earthworks site. (A)** Stratigraphic profile of the charcoal-rich Hopewell burn layer and typological age. Note the inclination and highly variable depths of the burn layer. The burn layer contains abundance peaks in microspherules, Pt, and Ir. **(B)** LiDAR image of the Krasnosky earthwork sample site. **(C)** Location of the Krasnosky earthwork site in southeastern Ohio. See also Table S2.

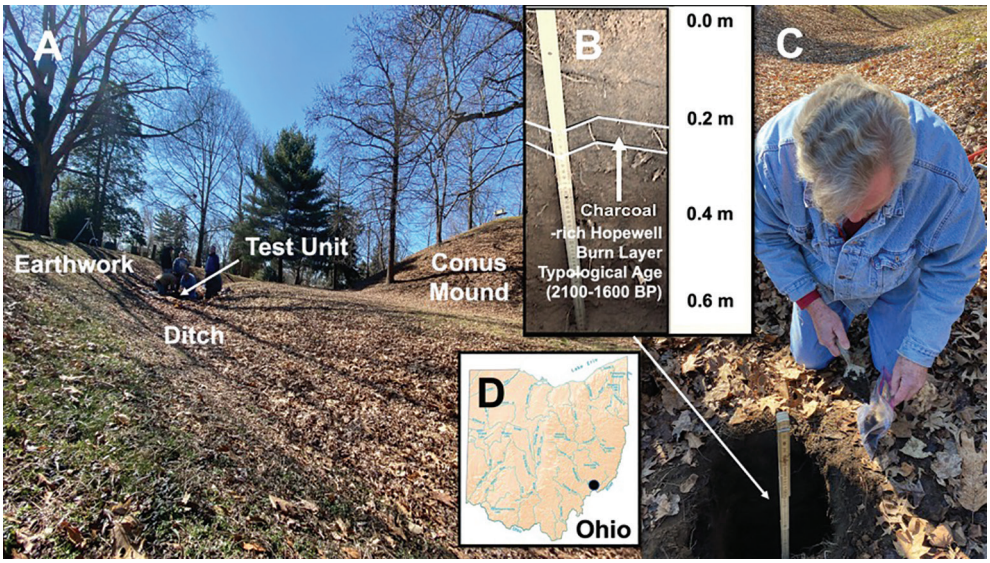

Figure 14: **Geographic and stratigraphic location of the Marietta earthworks geological sample site. (A)** Location of the test unit relative to the Conus Mound, earthwork berm, and ditch. Note the inclination and highly variable depths of the burn layer. **(B)** Stratigraphic profile of the charcoal-rich Hopewell burn layer and typological age. The burn layer contains abundance peaks in micrometeorites, microspherules, Pt, and Ir. **(C)** Excavation of the geologic test unit in the ditch surrounding Conus Mound. **(D)** Location of the Marietta earthworks site in southeastern Ohio. See also Table S2.

orientation. This shift in direction was likely produced by the prevailing west-to-east weather fronts that commonly pass across North America.

Stable carbon isotopes

Stable carbon isotope values were obtained on bulk organic matter from stratified sediments in a Hopewell-constructed reservoir at the Miami Fort village site (Table S20). The reservoir was part of a water management system constructed at the beginning of the Middle Woodland cultural period; ancestral Algonquians maintained it until European contact (Figure 34). Stable carbon isotope values were obtained from climosequences identified using X-ray diffraction (XRD) analysis of reservoir sediments [51]. They correlate

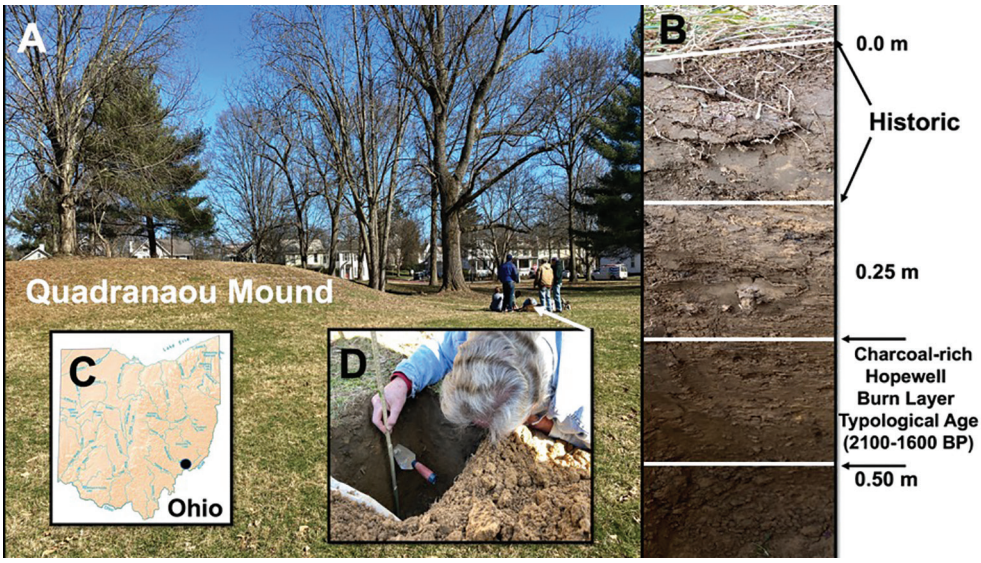

Figure 15: **Geographic and stratigraphic location of the Marietta earthworks archaeological sample site (304 m from the radiocarbon-dated Capitolium Mound). (A)** Location of the test unit relative to the Quadranaou Mound. **(B)** Stratigraphic profile of the charcoal-rich Hopewell burn layer and typological age. The burn layer contains abundance peaks in microspherules, Pt, and Ir. **(C)** Location of the Marietta earthworks site in southeastern Ohio. **(D)** The test unit next to the Quadranaou Mound. See also Table S2.

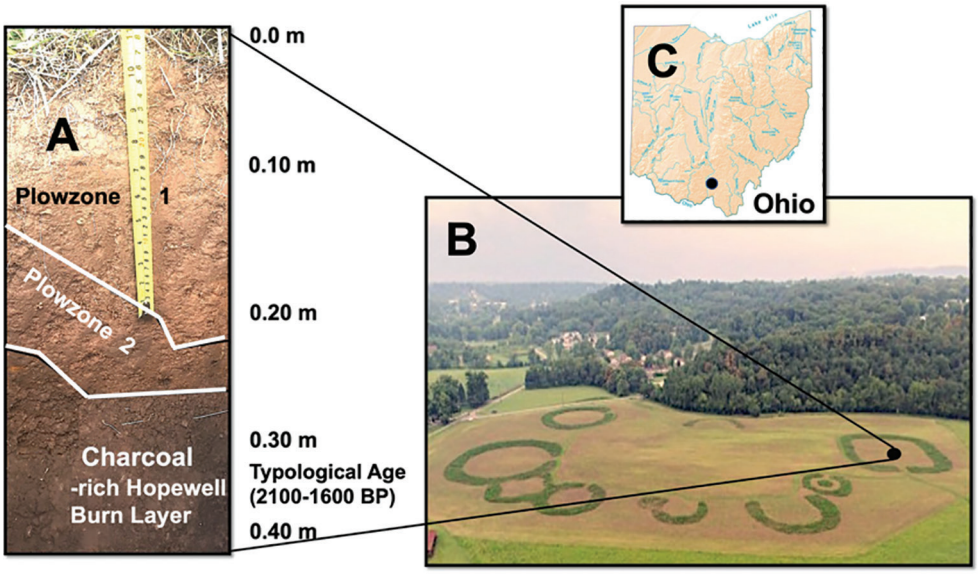

Figure 16: **Geographic and stratigraphic location of the Junction earthworks site. (A)** Stratigraphic profile of the charcoal-rich Hopewell burn layer and typological age. Note the inclination and highly variable depths of the burn layer. The burn layer contains abundance peaks in microspherules, Pt, and Ir. **(B)** Location of the test unit inside one of the Junction earthworks. **(C)** Location of the Junction earthworks sample site in southcentral Ohio. See also Table S2.

with the amount and type of vegetation cover in the reservoir catchment area.

Stable carbon isotope values from organic-rich sediments in the Hopewell reservoir show that the vegetation composition of the Miami Fort village site varied over time (Figure 33, Table S20). The $\delta^{13}C$ values from the Hopewell sediments ranged from −23.8 to −24.8‰ (N = 3) with an average of −24.2 ± 0.5‰. The $\delta^{13}C$ values of bulk organic matter from the post-Hopewell sediments ranged from −24.4 to −26.5‰ (N = 17) with an average of −25.3 ± 0.5‰. The stable carbon isotope values are indicative of a landscape dominated by C3 vegetation throughout the late Holocene. A significant change in the mix of plant species is indicated by a $\delta^{13}C$ value of −23.8‰, obtained from a stratum

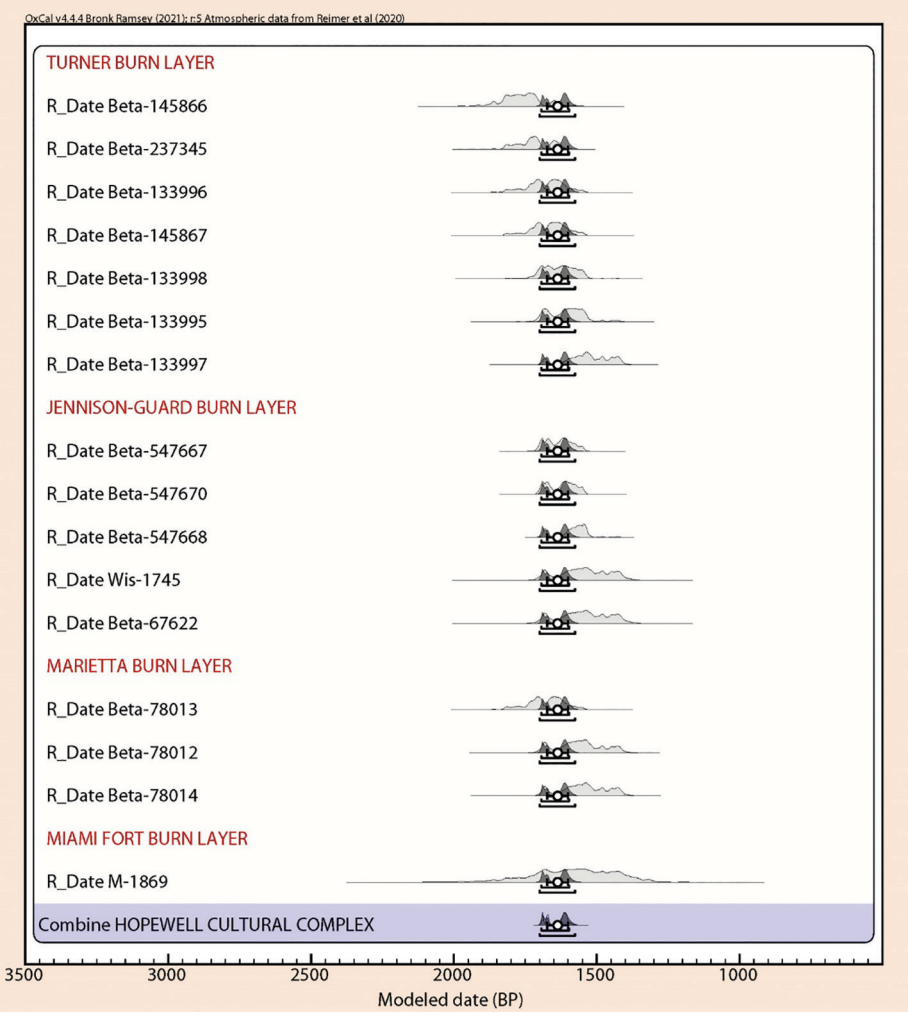

Figure 17: Test #1 of Synchronicity in OxCal. We used the Combine routine to determine that 16 of 17 radiocarbon dates likely represent a single event at 1635 ± 35 cal BP. The light gray curves represent unmodeled calibrated ages, and the dark gray represents modeled calibrated ages. Note that they overlap the modeled combined age, confirming the likelihood of synchronicity. The white dot beneath the curves equals the mean age. Progressively longer brackets beneath curves represent 68.3% and 95.4% confidence intervals (CI). The program performed two statistical probability tests to test the robustness of the model. Both the Acomb and chi-squared statistical tests show a high probability. For the table and OxCal code, see Table S11.

dating to the time of the proposed Hopewell airburst event (Figure 33). A value of 23.8‰ is within the range of C3 plants, but it is rare to see such positive values in terrestrial plants. One possible explanation is a mix of C3 terrestrial organics with either C4 terrestrial plants or aquatics/algae. The latter are known as "disaster species" that flourish after wildfires or other significant disturbances in the landscape [28], as proposed for the Hopewell sites.

Discussion

A suite of potential cosmic airburst or impact-related proxies, including micrometeorites, meltglass, microspherules, and elevated concentrations of platinum group elements (Ir and Pt), were found exclusively within the Hopewell strata of 11 archaeological sites in the Ohio River valley. These strata were comprised of burned Hopewell habitation surfaces, including the unambiguous remnants of burned wooden Hopewell structures, carbon-rich, and intensively heat-altered habitation surfaces (Figure 7).

Anthropogenic burning as possible causation

Numerous archaeological sites worldwide commonly contain evidence of bonfires, campfires, cremations, structural fires, and, in some cases, entire burned villages. However, for those sites that have been studied for impact-related proxies, all contain one burned layer with a suite of proxies and one or more burned layers without proxies (Ir, Pt, microspherules, and meltglass) [5, 11, 21, 33, 34]. In our

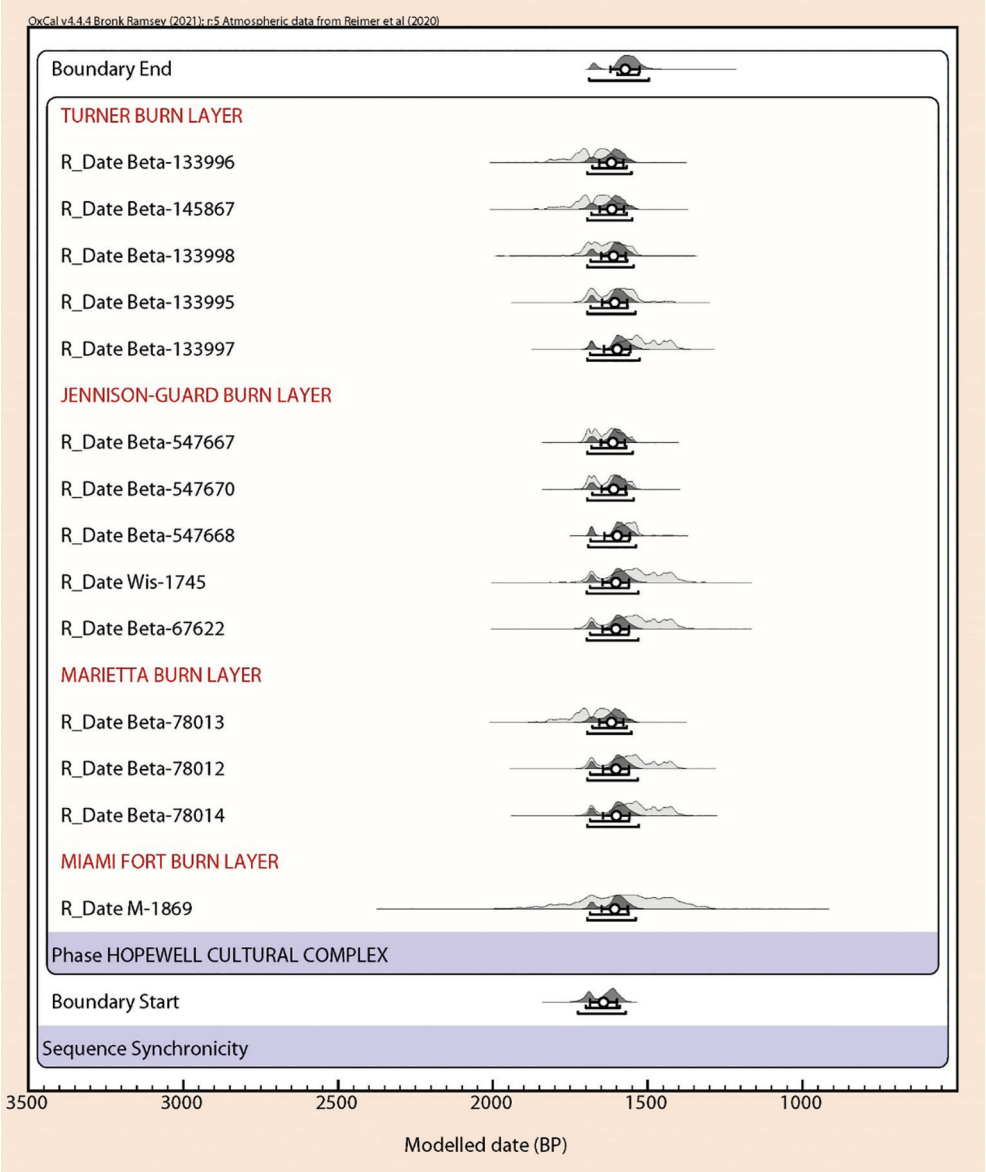

Figure 18: Test #2 of Synchronicity in OxCal. We used the Sequence routine and the Difference command to test the potential synchronicity of 17 radiocarbon dates on the Hopewell burn layer. Three dates were excluded as being too young or too old, but for the remaining 14 dates, the Sequence and Difference codes calculated the common age interval as ranging from 1600 ± 40 to 1615 ± 40 (1640-1570 cal BP), as represented by the black probability distributions. Light gray probability distributions represent the individual modeled YDB ages for each record; note that the unmodeled ages overlap the modeled probability distribution (black), confirming the likelihood of synchronicity. For the table and OxCal code, see Table S12.

research, we have found numerous cultural burn layers and fire features (e.g., hearths) at these and other Hopewell sites. Indeed, we have excavated dozens of Hopewell and other ancient Native American sites and have only found anomalous peaks in Ir, Pt, microspherules, and meltglass in coeval strata and have never observed these peaks above or below the synchronously dated occupation layer [35–37, 51–56]. This heterogenic distribution suggests a unique regional incident, such as the proposed airburst/impact event. It is important to emphasize that anthropogenic bonfires are exceedingly common in nearly all occupation layers in excavated villages, and yet, the only charcoal-rich deposits that contain this suite of proxies are in the proposed airburst/impact layer and not above or below it. If such proxies are caused by biomass burning alone, one would expect them to be ubiquitous in all burned layers, but they are not. Cultural layers above and below the Hopewell burn layer contain no detectable microspherules.

The Hopewell proxy-rich occupation layers from the Ohio River valley appear comparable to the Abu Hureyra

Table 2: EDS analysis of micrometeorites from the Turner site, Ohio.

NiFe Crystal and Olivine Group Elements									
Ni	**Fe**	**Mg**	**Ca**	**Mn**	**Al**	**P**	**K**	**Si**	**O**
0	41.59	4.25	0	0	0	0	0	3.33	50.83
0	29.82	11	0	0	0	0	0	9.97	49.2
0	33.19	9.63	0.62	0.66	0	0.35	0	8.98	45.38
0	33.19	9.63	9.63	0.66	1.09	0.35	0	8.98	45.38
0	28.42	12.72	0.52	0	0	0.33	0	11.8	45.78
0	30.14	12.42	0	0	0	0	0	11.67	45.77
0	59.78	2.66	0.7	0	0	0	0	3.09	33.67
0	23.48	16.55	0.33	0	0	0	0	11.5	48.07
0	29.23	13.34	0	0	0	0	0	9.81	47.62
0	41.55	8.5	0	0	0	0	0	10.04	39.76
0	4.26	0	1.28	0	1.03	0	0	2.59	24.22
0	0	2.01	4.2	0	8.42	0	1.73	18.2	44.83
0	39.68	5.22	0	0	0.94	0	0	4.28	38.33
0	33.35	10.45	0.76	0	0	1.62	0	7.33	46.48
0	39.23	3.23	2.88	0	0	5.84	0	2.79	46.03
0	38.14	3.16	2.83	0	0	5.74	0	2.71	45.2
0	33.35	10.45	0.76	0	0	1.62	0	7.33	46.48
0	38.14	3.16	2.83	0	0	5.74	0	2.71	45.2
0	0	0	0.25	0	5.03	0	0.41	14.6	42.09
0	53.86	0	0.28	0	1.15	0	0	2.76	37.13
0	0	2.01	4.2	0	8.42	0	1.73	18.2	44.83
0	66.44	0	0	0	0	0	0	0	33.56
0	0	0.85	0	0	3.99	0.26	0	9.18	43.38
0	0	0	0.25	0	4.23	0	0.41	14.6	42.09
0	0	0.85	0	0	3.99	0.26	0	9.18	43.38
0	9.08	1.74	1.12	0	9.69	0	1.84	23	53.53
0.6	15.68	14.77	0.59	0	4.32	0	0.78	17.79	45.47
0.79	33.51	10.8	0.42	0	0.68	0.33	0	8.07	45.4
0.95	35.57	2.2	0.16	0	0	0.2	0	2.5	44.81
1.18	31.14	15.12	0	0	0	0	0	8.93	43.62
1.33	38.33	6.91	0	0	3.16	0	0	9.32	39.64
1.36	83.65	0	0	0	0	0	0	0	14.99
1.36	83.65	0	0	0	0	0	0	0	14.99
1.96	47.86	0	0	0	0	0	0	10.55	37.41
3.23	55.06	0	0.28	0	1.18	0	0	2.85	37.39
3.53	45.67	3.21	1.56	0	0	3.89	0	2.78	39.36
27.03	44.02	1.61	0	0	0	15.29	0	0	10.6
27.55	44.69	1.66	0	0	0	15.5	0	0	10.6
0	14.74	23.8	0.21	0	0	0.67	0	13.29	47.28
0	12.32	26.88	0	0	0	0	0	15.83	44.97
0.53	11.91	26.3	0	0	0	0	0	15.3	44.36
0	9.3	26.69	0	0	0	0	0	18.37	45.64
0	14.74	23.8	0.21	0	0	0.67	0	13.29	47.28
0	14.57	25.37	0	0	0	0	0	18.32	41.74

High concentrations of Ni (orange) are inconsistent with most terrestrial deposits and consistent with known meteoritic material. Values highlighted in green from the Hopewell Turner site closely match known values for pallasites highlighted in yellow. Uncertainties are ± 10 wt%. *Note.* last results in yellow for olivine are from https://webmineral.com/data/Olivine.shtml.

site in Syria and the Tall el-Hammam site in Jordan [5, 33, 34]. For the impact proxies at Abu Hureyra, Moore et al. [33] performed furnace experiments demonstrating that bulk sediment can melt at ~1200°C. In contrast, temperatures of >1430°C are required to melt some observed grains at the Hopewell sites: chromferide ($Fe_3Cr_{0.4}$ = melting point, 2265°C); zircon ($ZrSiO_4$ = 1775°C); olivine ($(Mg,Fe)_2SiO_4$ = 1760°C); quartz (SiO_2 = 1720°C); titanomagnetite ($Fe^{2+}(Fe^{3+},Ti)_2O_4$ = 1625°C); magnetite (Fe_3O_4 = 1590°C); nickel-iron (NiFe = 1430°C). These temperatures are too high to permit melting in typical Native American campfires.

Moore et al. [33] also discussed previous research showing that midden or haystack fires cannot generate temperatures high enough to melt those grains. Similarly, Bunch et al. [24] found that midden fires, bonfires, and forest fires are not hot enough to melt magnetite into spherules. Otherwise, every forest fire would produce such spherules, and Bunch et al. [24] and Wittke et al. [27] searched for such deposits and

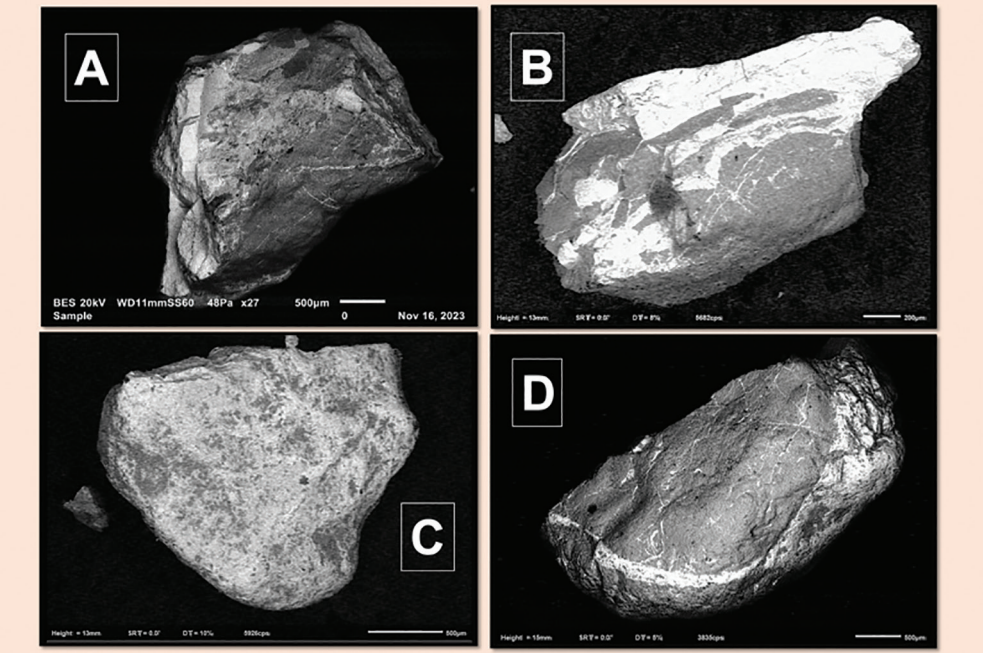

Figure 19: **SEM images of coarse sand-size stony-iron micrometeorites from the Turner site, Hamilton County, Ohio. (A-D)** Rounded pallasites, NiFe + $(Mg,Fe)_2SiO_4$). Note: these are individual, well-rounded microscopic micrometeorites, not ancient, angular Hopewell manufacturing debris.

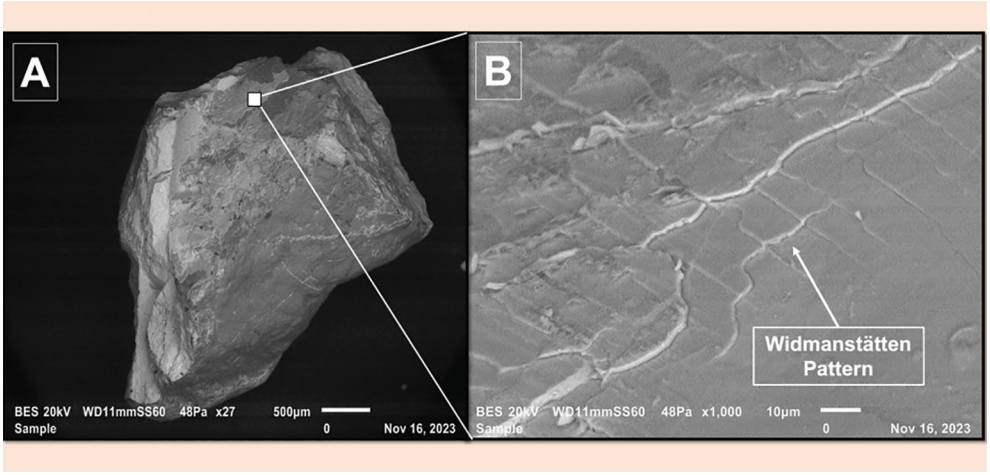

Figure 20: **Micrometeorite from the Turner site, Hamilton County, Ohio (see Figure 19A). (A)** SEM image of a coarse sand-size micrometeorite from the **(B)** SEM image of Widmanstätten patterns on the weathered surface of a coarse sand-size pallasite that has not been polished or acid etched.

found none in forest fires. A search of the available literature confirms that no forest fires have been reported to produce Fe-rich spherules such as those found at the Hopewell sites.

Based on previous evidence, we conclude that microspherules recovered from the Hopewell strata form at temperatures that greatly exceed those obtained in bonfires, midden fires, campfires, cremations, structural fires, and natural forest fires, as concluded for the Abu Hureyra site and Tall el-Hammam [5, 11, 33, 35]. The extreme temperatures that occur during impact events that form microspherules and meltglass do not occur under natural terrestrial conditions except for lightning strikes [5, 11, 33, 34]. However, lightning produces fulgurites, which were not observed in any Hopewell stratum and are easily distinguished from impact meltglass [5, 11, 33, 34].

Native American trade networks as possible causation

Trading of meteorites and subsequent reworking of those materials has been proposed to account for the high

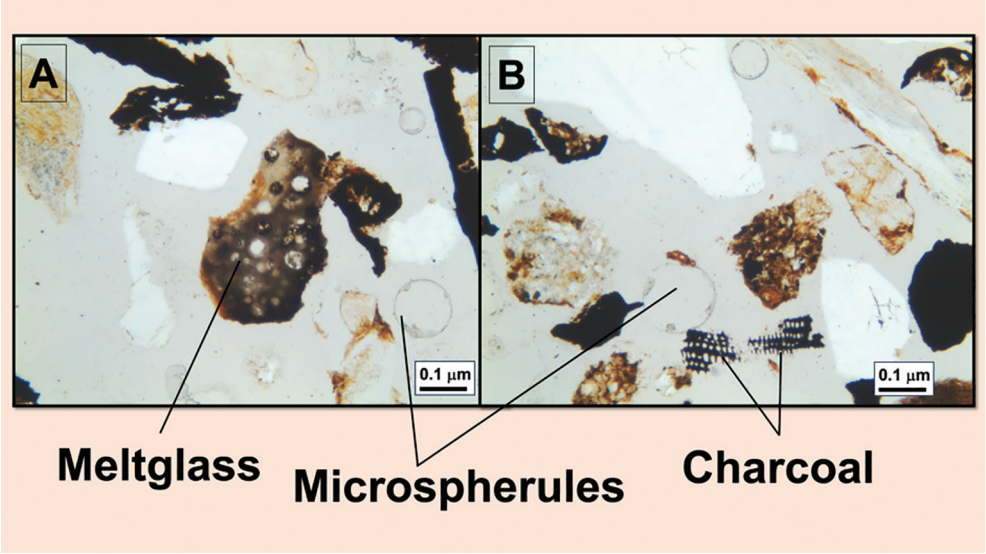

Figure 21: **Photomicrographs of a petrographic thin section of sediment samples from the charcoal-rich Hopewell burn layer at the Turner site. (A)** Photomicrograph of a petrographic thin section of meltglass and clear microspherules. **(B)** Photomicrographs of a petrographic thin section of clear microspherules and charcoal.

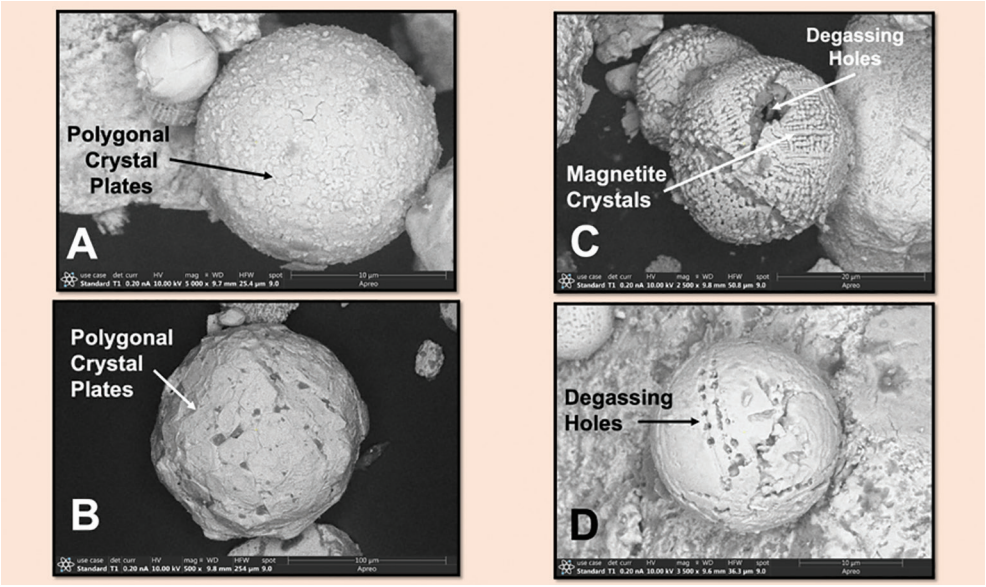

Figure 22: **SEM micrographs of microspherules from the charcoal-rich Hopewell burn sediments at the Turner sample site, Ohio. (A & B)** SEM micrographs of microspherules with "soccer ball-like" polygonal crystal plates. **(C)** SEM micrographs of microspherules with dendritic, "Christmas tree" magnetite crystal patterns. **(C & D)** SEM micrographs of microspherules with degassing holes.

concentrations of micrometeorites and PGEs at the Turner and Marietta sites. However, micrometeorites do not occur at the other nine Hopewell sites sampled. Likewise, meteorite trade cannot account for micrometeorites at the Turner site or the co-occurring peak concentrations of microspherules. In the Ohio River valley, meteorites only occur on Hopewell archaeological sites. If meteorites were valuable trade items, there should be evidence of trading meteorites in the archaeological strata of all cultural periods. However, there is no such evidence. Thus, a cosmic impact event is the most likely explanation for the co-occurring concentrations of these proxies.

Cosmic impact as possible causation

Although some of the melted Si-rich spherules at the Hopewell sites sampled may have been produced in bonfires, the Fe-rich spherules and other high-temperature melted grains could not have been produced that way – temperatures

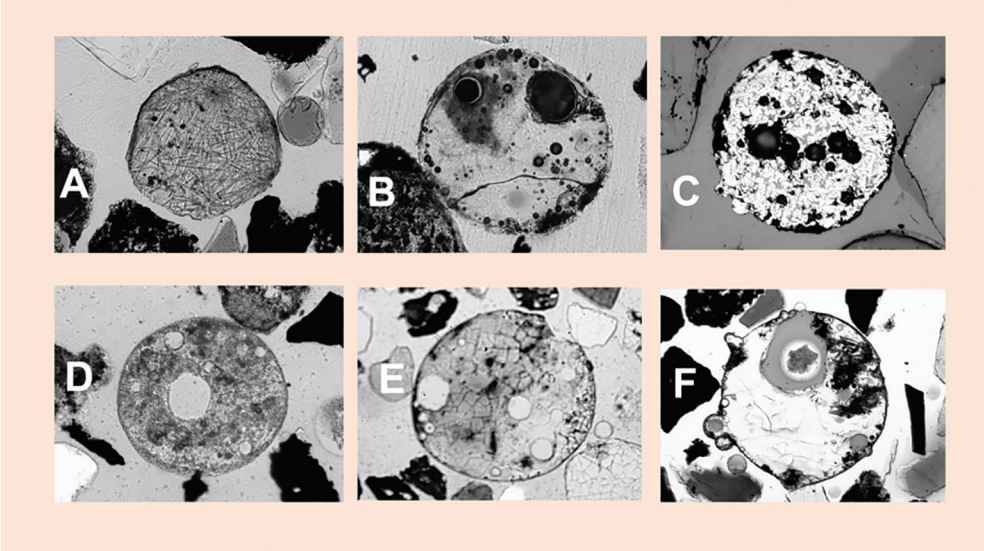

Figure 23: Photomicrographs of petrographic thin sections of Si-rich, glassy microspherules from the Hopewell stratum of the Turner village site, Hamilton County, Ohio. (A) Si-rich microspherule with needle-like rutile crystals (TiO_2, melting point 1843 °C, diameter 315 µm). **(B)** Microspherule with polygonal crystal textures and degassing holes (diameter 385 µm). **(C)** Microspherule with polygonal crystal textures and degassing holes (diameter 375 µm). **(D)** Microspherule with degassing holes (diameter 340 µm). **(E)** Microspherule with polygonal crystal textures and degassing holes (diameter 825 µm). **(F)** Microspherule with polygonal crystal textures and degassing holes (diameter 650 µm).

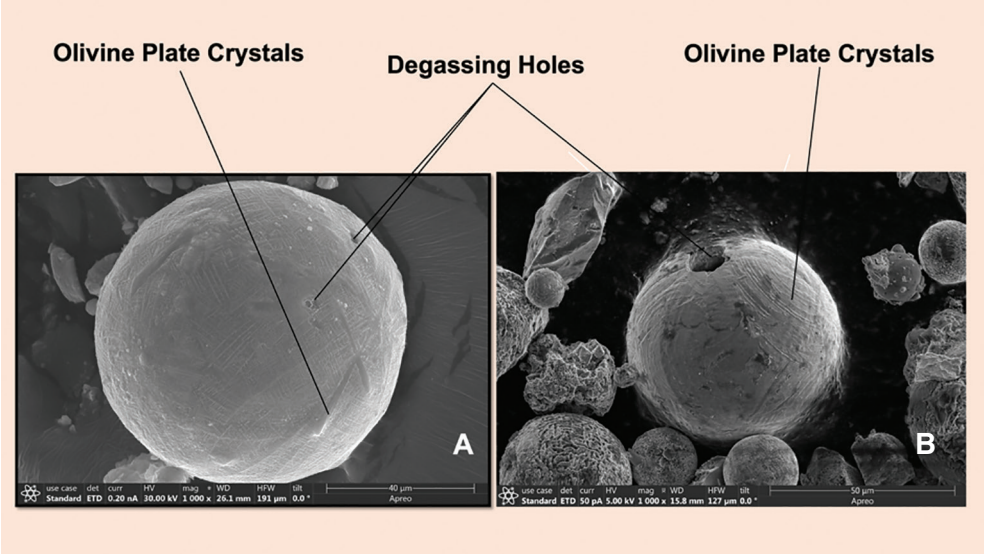

Figure 24: SEM micrographs of barred olivine microspherules from Hopewell sediments. (A) Miami Fort Village, Ohio. **(B)** Fosters earthworks, Ohio.

were too low. Thus, they require some other formation mechanism. The best explanation to account for the evidence is the occurrence of a cosmic impact event, most likely as multiple regional airbursts/impacts like those found associated with the Brenham/Haviland impact event in Kansas and the Eagle Station impact event in Kentucky [35, 36].

Based on the spatial distribution of Pt, Ir, microspherules, and meltglass from 11 Hopewell sites, we estimate the area affected by the airburst to be ~14,900 km^2. The epicenter of the proposed airburst was approximately ~500 km^2 and displays positive Pt anomalies > 3.0 ppb, positive Ir anomalies > 0.6 ppb, and peak abundances of microspherules.

Near-surface cosmic airburst and impact-related proxies occur in a stratum underlying the Milford airburst-shaped earthwork (Figure 10). The law of superposition dictates that the impact-related proxies likely predate the earthwork

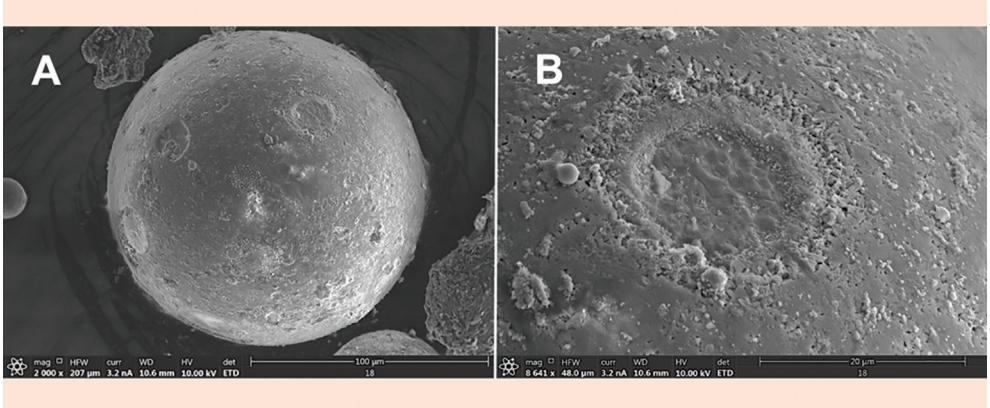

Figure 25: SEM micrographs of a pitted microspherule from the Hopewell sediments of the Turner site. (A) SEM micrograph of a large microspherule displaying numerous impact craters. **(B)** Close-up SEM micrograph of an impact crater on the surface of the largest microspherule (see SEM micrograph A).

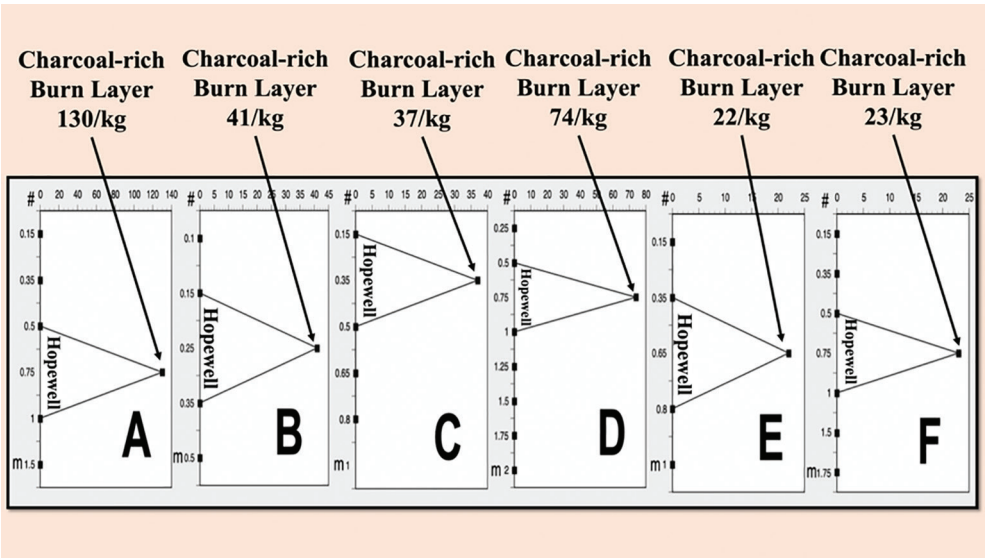

Figure 26: Quantity (#/kg) of microspherules in Hopewell archaeological sample sites by depth (m). (A) Turner site, Ohio. **(B)** Moundview site, Ohio. **(C)** Miami Fort, Ohio. **(D)** Jennison-Guard, Indiana. **(E)** Beech Tree site, Ohio. **(F)** Milford earthworks, Ohio. It is important to note that microspherules were not detected above or below the burn layer, even though the site was occupied before and after the event. This narrow distribution argues against formation through cultural biomass burning and other potential anthropogenic contamination.

construction. The compass angle of the geographic distribution of significant Pt and Ir anomalies is the same as that of the Hopewell-age Milford earthwork in Clermont County, Ohio. This common compass direction of the impact-related proxies and the airburst-shaped earthwork support the hypothesis that Native Americans witnessed the airburst and recorded their observation in a way comparable to the eyewitnesses of the Tunguska event.

Nolan et al. [23] argue that an impact event on a Native American village is statistically improbable and, therefore, questionable. However, 'improbable' does not mean 'impossible.' Earth's history is replete with hundreds of major impact events, all proposed to have been far larger than the one in the Ohio Valley. All of them were highly improbable events, yet they occurred. Thus, rarity is not a reasonable argument against an event's occurrence.

Napier and Clube [1, 6–8, 34] have provided an evidence-based model for such impacts. In addition, Moore et al. [34] attribute them to the hierarchical fragmentation of Giant comets called Centaurs, one of many <300-km-wide bodies in unstable orbits between the giant planets. Such large celestial bodies are proposed to undergo cascading disintegrations, some of which produced the Taurid Complex containing Comet Encke and ~90 asteroids with ~1.5- to 5-km diameters. When the Earth intersects the details of such large comets, the risk of multiple impact events across

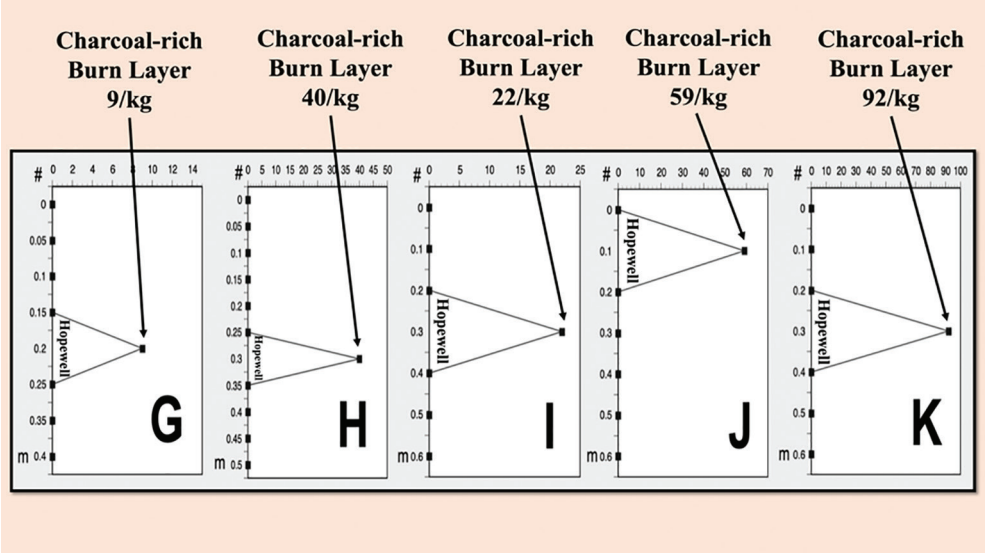

Figure 27: Quantity (#/kg) of microspherules in Hopewell archaeological sample sites by depth (m). (G) Marietta earthworks, Ohio. **(H)** Fosters Crossing, Ohio. **(I)** Krasnosky earthwork, Ohio. **(J)** Indian Fort Mountain, Kentucky. **(K)** Junction earthworks, Ohio. As at the sites above, microspherules were not detected above or below the burn layer.

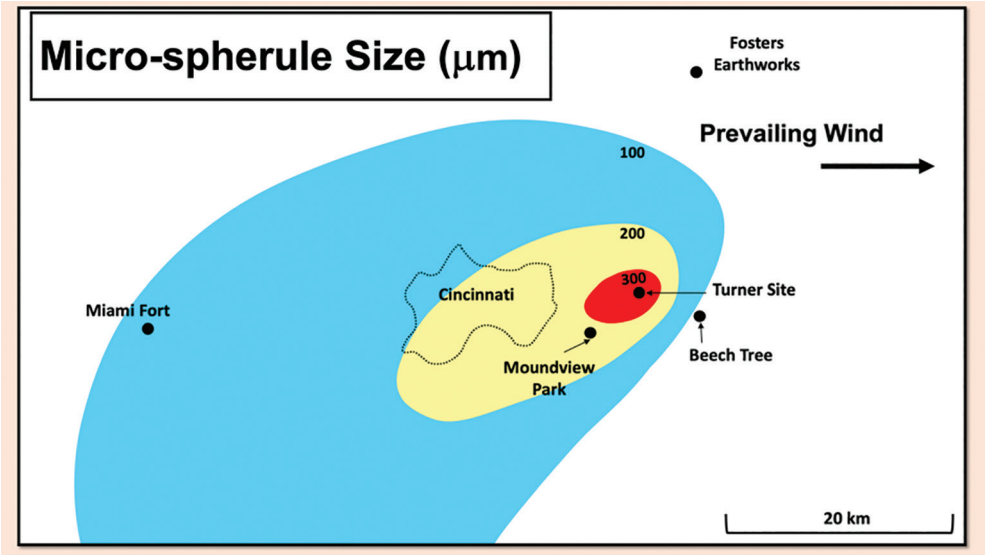

Figure 28: Geographic distribution of microspherules by size (mm) from the carbon-rich Hopewell burned strata sampled in the Ohio River valley. The red color indicates the proposed epicenter of the airburst event.

one Earth hemisphere increases substantially. Moore et al. [34] report that "*comets >100 km in diameter are expected to arrive from the Centaur region and enter short-period, Earth-crossing orbits about once every 20 to 60 kyr.... A 100 km-wide comet would have a mass 50-100 times that of the current near-Earth asteroid system, making such comets much more hazardous than the contemporary population of near-Earth asteroids when fragmenting in the terrestrial neighborhood.... The measured light curves of 34 of the associated asteroids and the mass and spread of the [Taurid] Complex ... indicate that the Complex represents the remains of a ~100-km-wide progenitor comet whose disintegration and dispersion has continued for at least the last ~20,000 years.*" This model could account for all the evidence we observed in the Ohio Valley and could result in a much larger statistical probability.

Anomalies in Pt and microspherules at control sites

To determine the distribution of this suite of proxies, we used the stratigraphic correlation between archaeological and non-archaeological units at two Hopewell

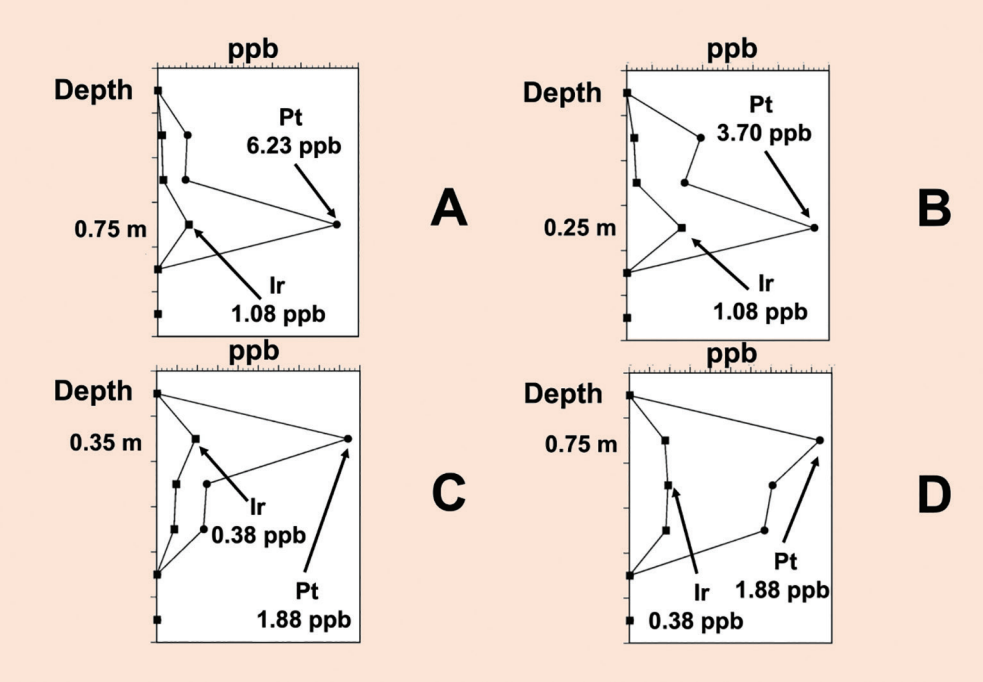

Figure 29: **Significant Pt and Ir anomalies in the carbon-rich Hopewell burned strata sampled in the Ohio River valley. (A)** Turner site, Ohio. **(B)** Moundview site, Ohio. **(C)** Miami Fort, Ohio. **(D)** Jennison-Guard site, Indiana.

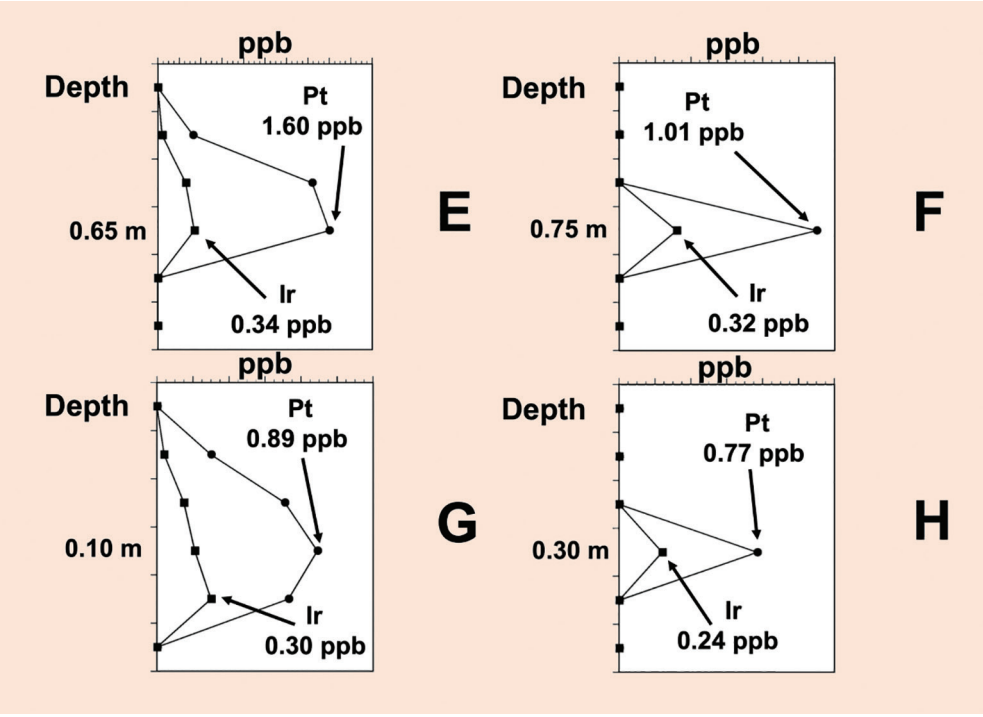

Figure 30: **Significant Pt and Ir anomalies in the carbon-rich Hopewell burned strata sampled in the Ohio River valley. (E)** Beech Tree site, Ohio. **(F)** Milford earthworks, Ohio. **(G)** Indian Fort Mountain, Kentucky. **(H)** Fosters Crossing, Ohio.

archaeological sample sites—the Jennison-Guard village site and the Marietta earthworks. We used a suite of criteria to conclude that strata in the archaeological and non-archaeological units had been thermally altered, including a visible change in soil color and texture, reduced soil porosity, and increased soil density. The thermally damaged

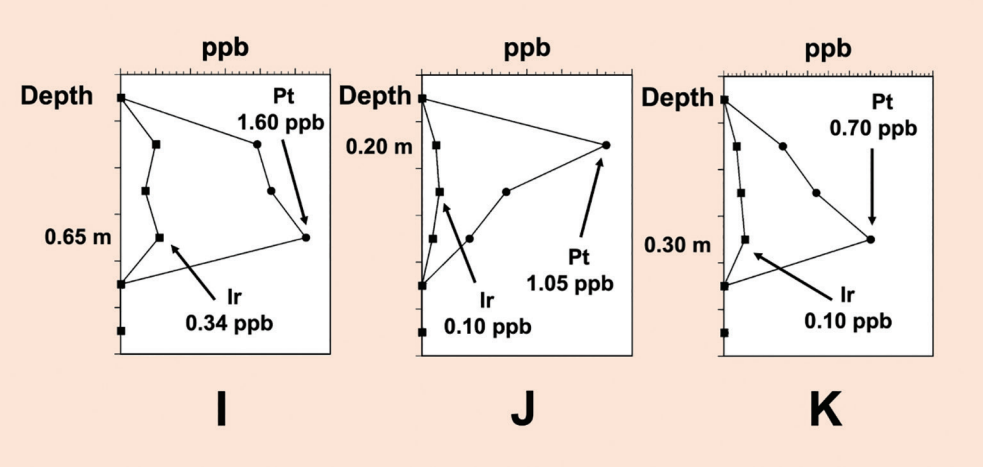

Figure 31: Significant Pt and Ir anomalies in the carbon-rich Hopewell burned strata sampled in the Ohio River valley. (I) Krasnosky earthworks, Ohio. **(J)** Marietta earthworks, Ohio. **(K)** Junction earthworks, Ohio.

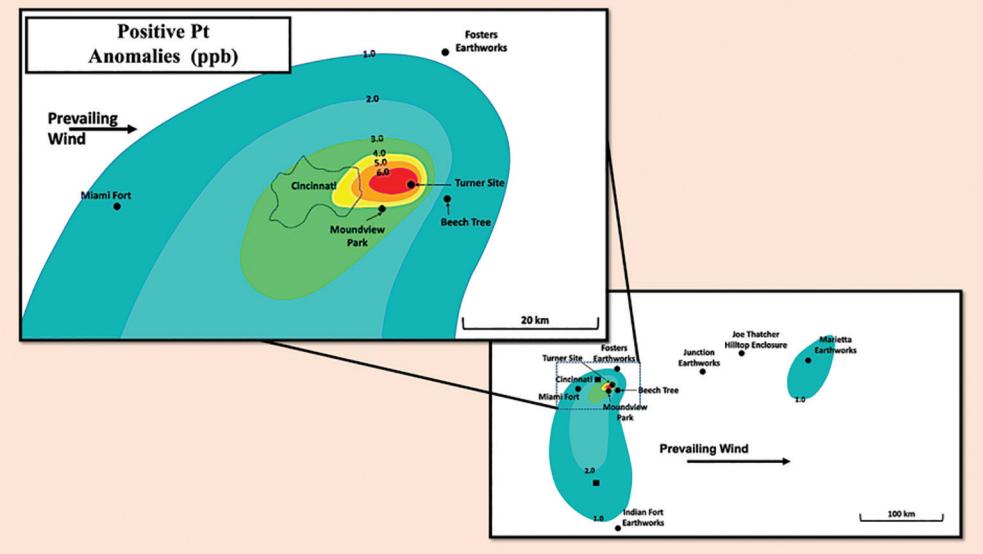

Figure 32: Geographic distribution of positive Pt anomalies from the carbon-rich Hopewell burned strata sampled in the Ohio River valley. The red color illustrates the proposed epicenter of the airburst event.

strata exhibited red and orange soil coloration from ferric oxide, a concentration of carbonized plant remains, a loss of absorbed and constitutional water, structural and compositional change in the hydrous silicates (i.e., clay), and decomposed carbonate minerals and rocks (e.g., aragonite, calcite, limestone, and micrite). The decomposition reaction of calcium carbonate ($CaCO_3$) to solid calcium oxide (CaO) and carbon dioxide gas (CO_2) occurs at a temperature of 1,200°C.

For the Jennison-Guard site in Dearborn County, Indiana, we excavated two units – one on an archaeological Hopewell village site located on a floodplain scroll bar of the Ohio River (Unit A) and a second unit on a nearby paleo-swale (Unit B), which served as a non-archaeological control (Figure 5). The units were separated by a linear distance of ~30 m. It is important to note that although the depths of the well-defined soil horizon boundaries varied widely across the units, we were able to use stratigraphy and radiocarbon dating to correlate the archaeological strata with the non-archaeological ones based on the presence of cosmic airburst and impact-related proxies recovered from the buried strata at both sites. This method is commonly used, often across vast distances, for diagnosing an impact spherule layer [47, 57].

To support our stratigraphic correlation at these two units (A and B), we obtained an AMS radiocarbon age of 1740 ±

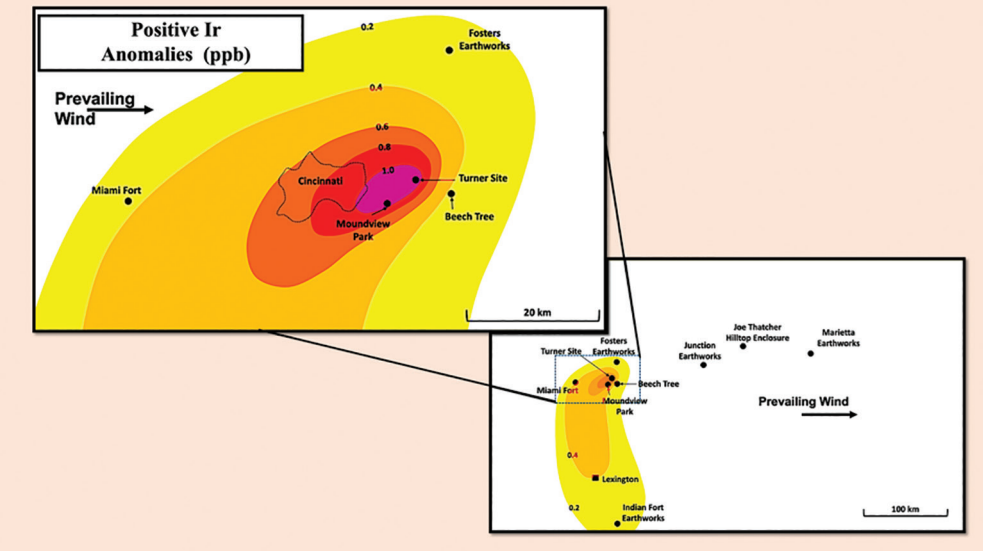

Figure 33: Geographic distribution of positive Ir anomalies from the carbon-rich Hopewell burned strata sampled in the Ohio River valley. The purple color indicates the proposed epicenter of the airburst event.

30 yr BP (1645-1544 cal BP, 62.9%) from the heavily burned, proxy-bearing stratum (paleosol, 2Aa) in Unit B, the paleo-swale at a depth of ~147.0 cm (Figure 5, Table 1, Table S1). No artifacts or archaeological features were identified in the paleo-swale's stratigraphy (Unit B). We also obtained three AMS radiocarbon ages from the heavily burned (Aa) archaeological stratum in Unit A located on a floodplain scroll bar: 1740 ± 30 yr BP (1705-1549 cal BP, 95%), 1680 ± 30 yr BP (1625-1518 cal BP, 81.7%), and 1630 ± 30 yr BP (1568-1409 cal BP, 95.4%). These calibrated radiocarbon ages are comparable to those previously obtained from the site (Table S1).

We conducted similar tandem unit excavations at the Marietta earthworks in Washington County, Ohio (Figures 14 and 15, Table S1). One unit, which exposed a Hopewell habitation surface, was excavated adjacent to the Quadranaou mound (~60 x 11 x 3 m) located 304 m from the radiocarbon-dated Capitolium Mound strata (Table S1). A second control unit was excavated in the center of a deep Hopewell-constructed ditch (~5 m wide, ~1 m deep) located between the Conus mound (~9 m) and surrounding earthen berm (~6 wide, ~180 m circumference). The locations of the two units were selected because the sites are separated by 968 m, and they contained surfaces that would have been exposed at the time of the airburst. Given that the ditch likely was filled with water at the time of the proposed airburst event, it would have been an ideal setting for the collection of accumulating carbon, magnetic microspherules, and PGEs.

We found that the Conus mound ditch contained an undisturbed Hopewell stratum and a sequence of subsequent natural infilling postdating the construction of the ditch (Figure 14). We found both significant Pt and Ir anomalies as well as microspherules co-occurring in the carbon-rich stratum from both the cultural and non-cultural units at the Marietta earthworks (Figures 14 and 15). The two units were separated by almost 1,000 m linear distance.

Social decline/reorganization at the end of the Hopewell cultural complex

Archaeologically, the Hopewell cultural complex is defined by the largest geometric earthen enclosures in the world, sophisticated hilltop water management systems, massive burial mounds, and ceremonial centers [16]. Distinctive reoccurring symbols are present on ceramic, ground-stone, and cold-hammered copper artifacts throughout the Ohio River valley and beyond [16]. Exotic Hopewell raw materials obtained from sources >2,400 km from archaeological sites suggest a widespread social network existed between the Atlantic Ocean and the Rocky Mountains and from Canada to the Gulf of Mexico [18]. These ancient cultural features and materials collectively suggest a stable, sedentary society with a political hierarchy [58, 59].

By ~1500 cal BP, the construction of world-class monumental landscape architecture had ended and was already in decline by ~1600 cal BP in southwestern Ohio [38]. While some hilltop water management systems, such as Miami Fort, continued to be maintained, new construction had ended [51]. Large ceremonial centers, over a hundred hectares in size, massive geometric earthworks, and burial mound complexes located along the Scioto and the Little and Great Miami rivers and their tributaries were no longer being built or expanded [58, 38]. The transcontinental movement of exotic raw materials such as obsidian and Knife River silicified lignite from distances >2,400 km ceased [18]. Temporally, the disappearance of these cultural hallmarks from the archaeological record has been used to define the

Table 3: Sample site locations and Ir and Pt data for Hopewell sediments.

Site	Burn Layer Depth (m)	Age cal BP at 95.4%	Age Typological (cal BP)	14C Sample Depth (m)	Pt-Ir Sample Depth (m)	Ir (ppb)	Pt (ppb)	Distance from Turner
Turner, OH, Hamilton Co.	0.65-1.55	1940-1470	2100-1500	1	0.75	1.08	6.23	0
Moundview, OH Hamilton Co.	0.11-0.32		2100-1500		0.25	1.08	3.7	5.5
Miami Fort, OH Hamilton Co.	0.20-0.65	1700-1405	2100-1500	0.91-1.59	0.35	0.38	1.88	44
Jennison-Guard, IN, Dearborn Co.	Unit A 0.75-1.2	1815-1305	2100-1500	0.55-0.85	0.75	0.38	1.88	47
	Unit B 1.4-1.5		2100-1500					
Beech Tree, OH, Clermont Co.	0.65-0.70		2100-1500		0.65	0.34	1.6	6.2
Milford Earthworks, OH Clermont Co.	0.74-0.89		2100-1500		0.75	0.32	1.01	4.3
Indian Fort Mtn, KY, Madison Co.	0.07-0.22		2100-1500		0.1	0.3	0.89	178
Fosters Crossing, OH, Warren Co.	0.25-0.40		2100-1500		0.3	0.24	0.77	20.5
Krasnosky Earthwork, OH, Hocking Co.	0.10-0.42		2100-1500		0.3	0.11	0.53	154.5
Marietta Earthworks, OH Washington Co.	Conus		2100-1500		0.2	0.1	1.05	248.1
	0.19-0.25							
	Quad-ranaou							
	0.30-0.50							
Junction Earthworks, OH								
Ross Co.	0.27-50		2100-1500		0.3	0.1	0.7	117.7
Crustal Abundance						0.2	0.5	
SARM-7 (mg/kg)						0.074 ± 0.012	3.74 ± 0.0045	

Note. the depths of 14C samples are sometimes different than those of Pt-Ir samples due to the high variability of strata depths between and within the same profile. Nevertheless, each burn layer contains Hopewell artifacts co-occurring with abundance peaks in microspherules, Pt, and Ir with few to none above or below, including in layers with other cultural artifacts. Uncertainties for Pt and Ir are ± 10 wt%.

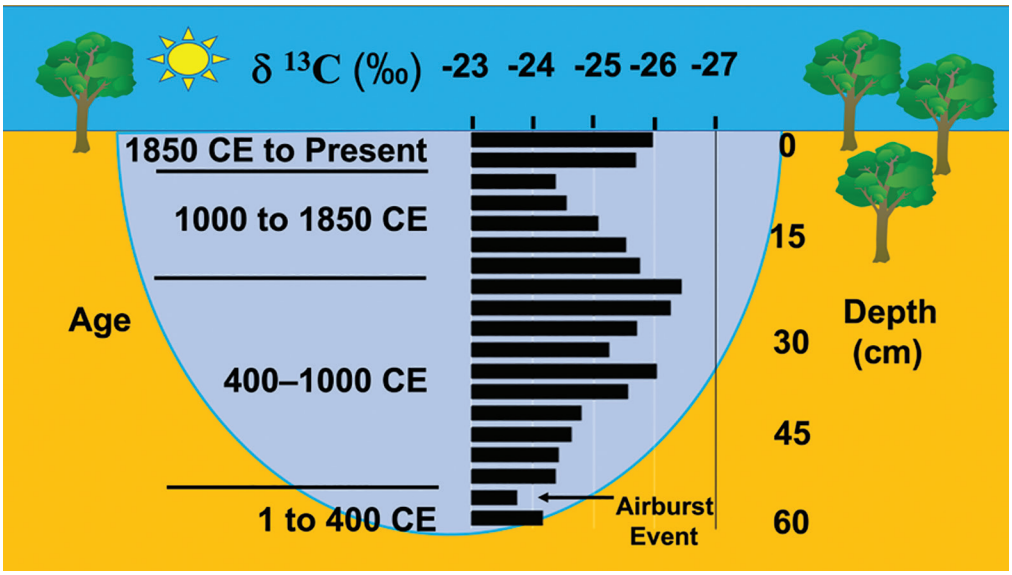

Figure 34: Stable carbon isotope values and ages by depth in a Hopewell-constructed reservoir at the Miami Fort village site, Hamilton County, Ohio. The δ ^{13}C values indicate a significant change in the composition of C3 vegetation (–23.8‰) at the time of the proposed Hopewell airburst event.

end of the Hopewell cultural complex [18, 60]. The disappearance of these archaeological hallmarks suggests that a social collapse, economic decline, or political reorganization occurred in the Ohio River valley by ~1500 cal BP [60].

For more than 200 years, archaeologists have speculated on possible causes of the socio-political end of the Hopewell cultural complex [61, 62]. Various Eurocentric theories have been proposed to explain the disappearance of distinctive Hopewell cultural traits from the archaeological record, including economic collapse, intrusion of rival cultures, migration, and warfare [58, 60]. Economic collapse from immigration and fighting between one or more rival cultures has been the longest-championed and most popular theory. It is based on three assumptions: (1) there was a socio-political breakdown in the long-distance spheres of interaction, (2) there were armed conflicts that resulted from an immigration of one or more rival cultures into the Ohio River valley, and (3), hilltop Hopewell earthworks were defensive fortifications that served as places of refuge during times of warfare [63, 64].

There are multiple problems with the theory of economic collapse from immigration and fighting between one or more rival cultures: (1) hilltop earthworks are inadequate for defensive purposes, (2) hilltop earthworks were built for ceremonial purposes and water management, and (3) hilltop earthworks appear at the beginning, rather than the end, of the Middle Woodland cultural period [65–68].

Two Bayesian tests indicate that the proposed impact event was synchronous across at least four Hopewell sites. In addition, the presence of abundance peaks in micrometeorites, microspherules, Ni, Pt, and Ir suggests that the event occurred synchronously across the study area. Pan-globally and through time, natural catastrophes such as cosmic airburst events have led to socio-political decline and reorganization [1, 6–9, 49]. We propose that the occurrence of a cosmic airburst near the end of the Hopewell cultural complex is a far more plausible explanation for socio-political decline than the previously proposed Eurocentric theories. Transgenerational oral histories of Indigenous peoples living in the Ohio River valley provide what Vine Deloria Jr. called "eyewitnessed" accounts of a cosmic airburst [69].

Indigenous oral histories in support of cosmic impact events

Transgenerational astronomical knowledge is crucial to the survival of Indigenous peoples, and this knowledge is communicated through symbols in art, ceremony, dance, music, and song and through landscape architectural artwork (e.g., earthworks), all of which are effective ways to communicate transgenerational Indigenous knowledge [70]. Hopewell earthwork symbolism provides a visual representation of human-landscape relationships so that anyone versed in the symbolism of the Indigenous culture that created the earthworks can derive a consistent narrative from them [71, 72]. Both the Turner and nearby Milford sample sites in southwestern Ohio contain unique airburst-shaped Hopewell earthworks (Figures 2, 10, 35, and 36). They are located within 3.75 km from one another. There are no other known Hopewell earthworks like them, suggesting they represent unique landscape symbols tied to a specific transgenerational narrative [72].

The shape of the elevated circle and graded way of the Turner earthworks closely resembles the photographs of the 9,100-metric ton, low-angle, Chelyabinsk meteor that came into view over Russia on February 15, 2013 (Figure 36C).

The Chelyabinsk meteor appeared brighter than the sun, generated intense heat, and it was visible from 100 km away [73]. The meteor exploded in an airburst ~29.7 km above the Earth's surface [73].

The Milford earthwork is very similar to the hand-drawn sketches made by eyewitnesses of the ~12-megaton Tunguska impact event on June 30, 1908, in Yeniseysk Governorate, Russia (Figure 36C) [74, 75]. Eyewitness drawings of the Tunguska impact event depict a red ball, twice as large and as bright as the sun with a fiery broom emitting sparks behind it [74, 75]. Given the remarkable similarity with the eyewitness drawings of the Tunguska impact event, it is reasonable to speculate that the Milford earthwork is also a visual record of a comparable impact event (Figure 36A-C).

The writings of Vine Deloria Jr. and Native American oral histories support the interpretations of the Turner and Milford earthworks as physical representations of an eyewitnessed cosmic event. He argued that Native American symbolism and oral histories contain transgenerational knowledge of past cosmic impact events [69]. He maintained that they are deeply rooted in eyewitnessed events. Indeed, there are intertribal accounts for the same or similar impact events [49]. The Anishinaabe have an oral history of Genondahwayanung, the Long-Tailed Heavenly Climbing Star, which was as bright as the sun with a long, wide tail that destroyed Anishinaabe villages [48]. The Anishinaabe oral history emphasizes that this was not the first occurrence of Genondahwayanung, nor would it be the last [49].

Oral histories of the Myaamiaki tell of a star that was as bright as the sun and crossed the sky. They called it Lenipinšia, which means horned serpent [76]. They observed it dropping rocks from the sky before it plummeted into a river, consistent with the observed behavior of bolides that typically break into multiple fragments due to intense friction after impacting Earth's atmosphere. These stories are consistent with the comet/meteor-shaped earthworks at the Turner and Milford sites (Figures 10, 35, and 36).

The Adawe described one cosmic impact event on a day when the sun fell from the sky [48]. The Wyandotte remember an apparent impact event as a time when a black cloud rolled across the sky [76]. The Haudenosaunee spoke of the impact event in which Dajoji, the Sky Panther, tore down forests [77]. The Shawano and Piqua made similar observations, which they called Tekoomsē, meaning blazing comet, also known as the Sky Panther [78–80]. The name Tekoomsē was given to Tecumseh in 1769, within the first year of his life, when comet C/1769 P1 was visible to the naked eye [79, 80]. It is also noteworthy that Comet C/1811 F1 is known as Tecumseh's Comet because he believed the comet was a good sign for his intertribal plan to expel the settler colonists [79, 80].

Micrometeorites and images of horned serpents (Sky Panthers) were collected from the same Hopewell contexts at the Turner site [19]. For example, pallasites were found along with two carved horned serpents in Mound 4 (Figure 37). One was carved from chlorite mica with a freshwater pearl eye and covered in red ochre, and the other was manufactured from a red heat-altered carbonate-rich shale [19]. Their

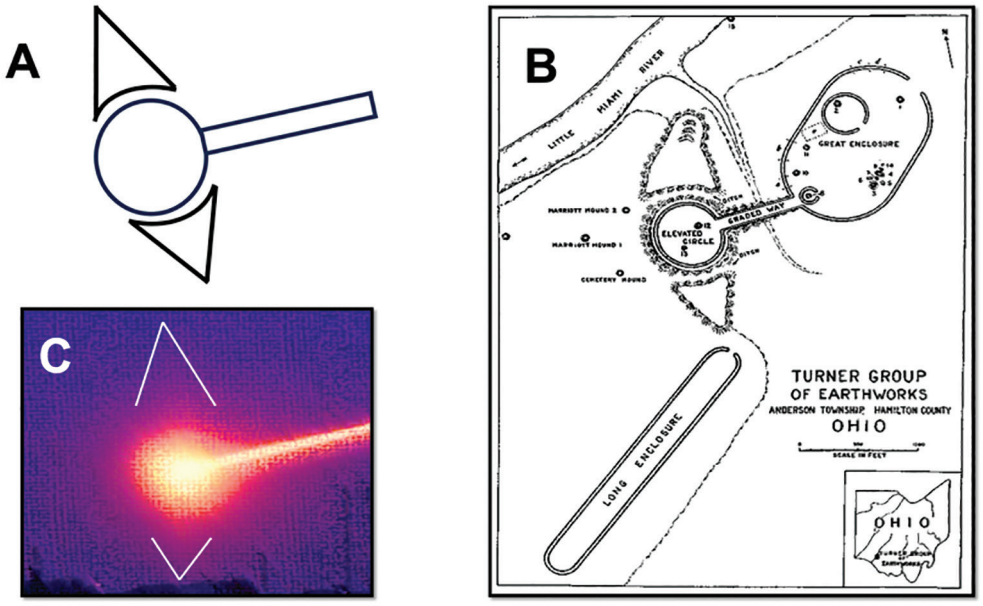

Figure 35: The Turner earthworks compared to the Chelyabinsk meteor. (A) The Elevated Circle and Graded Way of the Turner earthworks. **(B)** The 1887 Hosbrook map of the Turner earthworks revised by Starr in 1960. **(C)** The Chelyabinsk meteor with white lines illuminating features are comparable to those of the Turner earthworks [73].

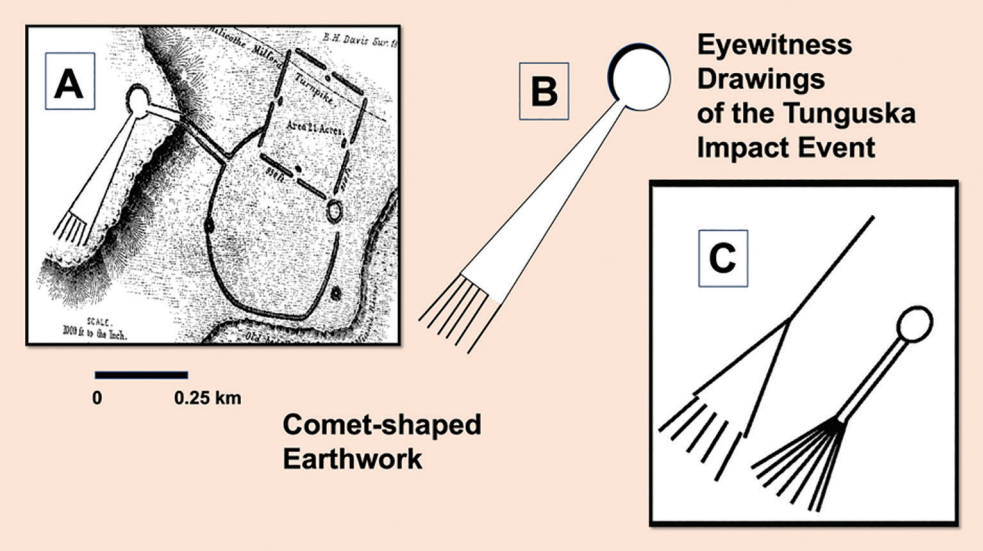

Figure 36: The Milford earthwork and eyewitness drawings of the Tunguska impact event. (A, B) The 1847 Ephraim George Squier and Edwin Hamilton Davis map of the Milford earthwork. **(C)** Eyewitness drawings depicting the June 30, 1908, Tunguska impact event in Yeniseysk Governorate, Russia [74, 75].

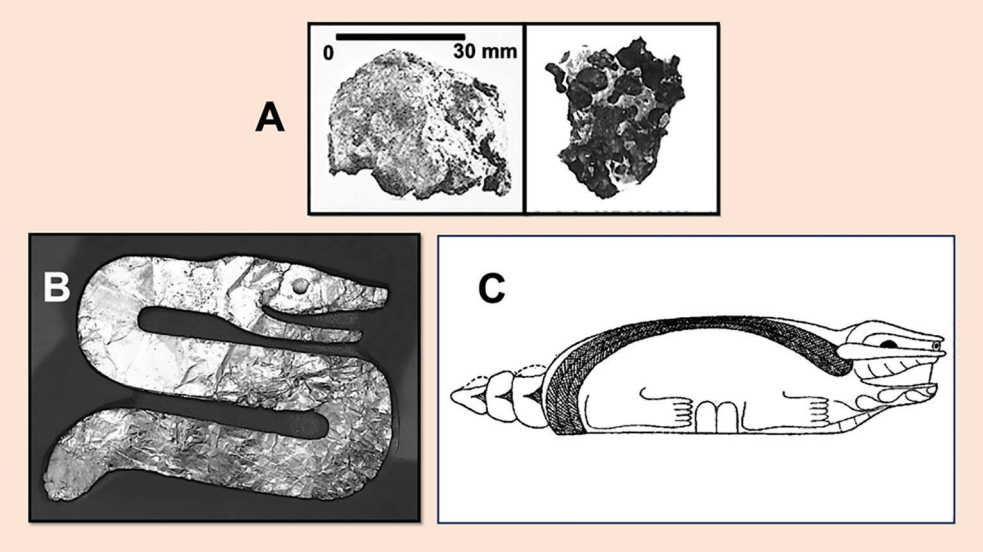

Figure 37: Micrometeorites and horned serpents (Sky Panthers) from the Mound 4 of the Hopewell Turner site [19]. (A) Pallasites excavated in direct association with horned serpents (Sky Panthers) from Mound 4 of the Turner Hopewell site. **(B)** A Sky Panther, also known as a horned serpent, carved from chlorite mica with a freshwater pearl eye and covered in red ochre. **(C)** A Sky Panther, also known as a horned serpent, manufactured from a red heat-altered carbonate-rich shale.

co-occurrence suggests a first-hand understanding of the Sky Panthers' relationship with the meteorites.

Conclusion

Anomalous abundance peaks in micrometeorites, melt-glass, melted microspherules, Ni, Pt, and Ir occur together in Hopewell cultural strata in the Ohio River valley. These peak abundances only occur in a dark, charcoal-rich burn layer and are not found above or below that layer. We propose that this suite of proxies is best explained as representing a cosmic airburst event. Identifying these proxies is an effective tool for diagnosing a cosmic impact or airburst event, and they also provide a useful chronostratigraphic marker in archaeological and non-archaeological contexts.

Airbursts are by far the most frequent cosmic events that have affected the Earth and are known to have caused structural damage and contributed to cultural downturns. NASA has concluded that a Chelyabinsk-sized meteor impacts the Earth every 10 to 100 years on average over a millennium, based on our constantly evolving understanding of the population of comets and asteroids [81]. Even a relatively small impact event or airburst could have had the ability to destroy several villages and negatively impact the Hopewell socio-political system. Multiple simultaneous airbursts/impacts from a fragmented comet or asteroid are capable of regional devastation.

Following the proposed impact event, Hopewell sites at or near the epicenter of the airburst, such as Turner, Moundview, Beech Tree, Milford, and Foster, were abandoned. We found no evidence of subsequent Indigenous occupations at these sites. Elsewhere in southwestern Ohio, the ancient mega-cultural features, including monumental landscape architecture, transcontinental movement of raw materials, and extensive burial mound and ceremonial centers, began to decline ~1600 cal BP and eventually disappeared altogether in the Ohio River valley by ~1500 cal BP. This age range includes the Bayesian-derived age range of the impact event (1640-1570 cal BP). These changes suggest a widespread social decline or reorganization in this region and possibly beyond. While many previous theories have been offered to explain the "end" of epic Hopewell earthwork building, none address all the relevant issues. Based on the currently available evidence, we suggest that a cosmic airburst/impact event may have triggered the decline or reorganization of what archaeologists call the Hopewell cultural complex.

Methods

Field methods

Sediment samples were obtained from archaeological units and trenches, which were hand excavated using standard archaeological procedures. Stable carbon isotope samples were extracted using a split-spoon, 5-cm diameter solid sediment core, and a hand-operated drop hammer. Soil horizons and stratigraphic boundaries were defined in the field based on color, texture, structure, and pedogenic features and confirmed in the lab with particle size analysis and Munsell soil color charts. The location of all archaeological features, sediment cores, excavation units, and trenches were recorded in the field using a hand-held GPS.

ICP-MS analysis

All ICP-MS analyses were conducted at the University of Georgia, Center for Applied Isotope Studies. They prepared all solutions gravimetrically with ultra-pure deionized (18MΩ) water and certified trace metal grade acids. Certified trace-metal grade HNO_3 (67-70% w/w) and HCl (36% w/w) were purchased from Fisher Scientific (USA). Indium 1000 ppm and 10-ppm multielement standard CMS-2 were purchased from Inorganic Ventures (USA). An Iridium 10-ppm standard was purchased from Ricca (USA), and a Pt 1000-ppm standard was purchased from SPEX CertiPrep (USA). SARM-7 reference material (RM) is from SACCRM (South Africa). Certified values are 0.074 ± 0.012 mg/kg Ir and 3.74 ± 0.0045 mg/kg Pt. PFA digestion vessels were from Savillex (USA). Metal-free polypropylene centrifuge tubes were from VWR (USA).

A large sub-sample was dried in an oven at 60 °C for 48 hours and then ground in a porcelain mortar and pestle. Clean, dry Savillex vessels were accurately weighed to 4 decimal places on an analytical balance, whose calibration is checked daily. A 200 mg sub-sample of the ground sample was transferred to Savillex and weighed. Exactly 200 µl deionized water was pipetted into Savillex for use as method blank and weighed. Exactly 1 ml of freshly prepared aqua regia (4:1 v/v HCl:HNO_3, equivalent to 3:1 mol/mol) was added to each Savillex. The Savillex capped and vortexed gently. It was then placed on a hot block with caps loosened and heated at an internal temperature of 90 °C for 1 hour. Samples were allowed to cool, the caps were tightened, and the Savillex weighed. The contents of the Savillex were transferred to a pre-weighed centrifuge tube, which was then centrifuged to prevent the transfer of particulates.

An aliquot of the supernatant was transferred via micropipette to a pre-weighed centrifuge tube, which was then weighed again. The aliquot was diluted with deionized water, vortexed, and weighed again. This diluted solution was run on the ICP-MS. The remaining sediment was dried and weighed to determine the proportion of the original sample that had been digested. Instrumentation included a Thermo X-Series II (Thermo Fisher Scientific, Germany) with peristaltic pumps and Cetac ASX 520 auto-sampler (USA). The cyclonic spray chamber was maintained at 3 °C to minimize oxide formation. Ion lens voltages, nebulizer flow, and stage positioning were optimized daily using a tuning solution to maximize ion signal and stability while minimizing oxide levels (as CeO+/Ce+) and doubly charged ions (as Ba2+/Ba+). The ICP-MS was run in kinetic energy discrimination mode (KED) using a collision/reaction cell with a custom 8% H_2 in He gas (Airgas, USA) and negative pole and hexapole biases separated by 3 V. This is done to remove polyatomic interferences, such as oxides. KED mode was optimized to minimize the signal on m/z 75 of an HCl blank while maximizing 75As signal of an As solution in HCl. Internal standard: 20-ppb indium solution supplied by Trident inline mixing Tee (Glass Expansion, USA). ^{115}In was used for drift correction.

A blank consisting of 5% w/w HCl was used to calibrate and calculate the detection limits. Pt: 0.001, 0.01, 0.1, 1, 10, 100 µg/kg calibration solutions prepared in 5 % HCl. Ir: 0.001, 0.01, 0.1, 1, 10 µg/kg calibration solutions prepared in 5 % HCl. QC standard: 0.01 and 0.1 µg/kg solutions of

CMS-2 prepared in 5 % HCl for continuing calibration verification were run every 12 samples and at the beginning and end of the analysis. Preferred isotopes measured for analyte elements are listed in report (193Ir and 195Pt). Alternate isotopes of the analyte elements (^{191}Ir and ^{194}Pt) were also monitored. All samples and standards run in triplicate, except for the blank, which was run in triplicate for the calibration and ten times for the LOD determination. QC standards were within 80-120% recovery.

Dilution factors were calculated from the mass of the sub-sample digested, the mass of the digested solution, the mass of the aliquot taken, and the mass of the final dilution. The ICP-MS software, PlasmaLab (Thermo Fisher Scientific, Germany), calculated the concentration of each replicate of the diluted solutions using the calibration curve. The data were exported to Excel (Microsoft, USA), where the three replicates were averaged. Limits of detection were calculated as 3 times the standard deviation of the 10 replicates of the blank. Concentrations were checked against the LOD. Any that were found to be less than the LOD were reported as such. If any Pt or Ir was found in the MB, it was subtracted from the samples and reference materials. The solution concentration was multiplied by the dilution factor to determine the concentration in the dry solid sample. The concentrations of the samples and RM were reported, along with the proportion of samples digested.

Stable carbon isotope analysis

All Stable carbon isotope analyses were conducted at the Center for Applied Isotope Studies at the Reston Stable Isotope Laboratory, United States Geological Survey. They prepared samples for carbon isotopic analysis and were powdered via a ball mill grinder until the aliquot was reduced to a fine enough grain size to analyze on an elemental analyzer. Samples were converted to CO_2 with an elemental analyzer; gases were separated with a GC, and the gases were analyzed with a continuous flow isotope ratio mass spectrometer. Isotopic reference materials are interspersed with samples for calibration. Relative carbon isotope ratios are reported in per mil relative to VPDB (Vienna Peedee belemnite) and normalized on a scale such that the relative carbon isotope ratios of L-SVEC $LiCO_3$ carbonate and NBS 19 $CaCO_3$ are −46.6 and +1.95 per mil, respectively. Stable carbon-isotope results are reported on the VPDB-LSVEC scale via normalization with other internationally distributed isotopic reference materials. The 2-sigma uncertainty of carbon isotopic results is 0.5 per mil unless otherwise indicated, meaning the values are within an uncertainty of 95 percent.

Micrometeorites, microspherules, and meltglass

Micrometeorites, microspherule morphologies, and meltglass from Hopewell strata were extracted in the Ohio Valley Archaeology Laboratory at the University of Cincinnati based on previously published protocol [3, 25]. Sediment samples were collected from well-dated, stratified archaeological sites and labeled by depth and chronostratigraphic context. A 450-g aliquot was weighed for each sample, and a slurry was created from a mixture of bulk sediment, water, and a deflocculant (hydrogen peroxide, H_2O_2). The magnetic grain fraction was then extracted using a rare earth neodymium magnet. Additional sieving was used to collect non-magnetic melt-glass and microspherules. Microscopic meteorites, magnetic microspherule morphologies, and meltglass were identified using light microscopy, petrographic thin-section analysis, and scanning electron microscopy. An EDS system was used to identify the elemental composition of the microspherules. SEM and EDS were accomplished in the Advanced Materials Characterization Center at the University of Cincinnati, the Electron Microscopy and Surface Analysis Lab at the University of Utah, and Elizabeth City State University.

Bayesian analysis

Age-depth model

This description here and in the text is adapted from Kennett et al. [82]. We calibrated all dates using the calibration curve using IntCal20 within OxCal v4.4.4, r:5 [83, 84], and then calculated age models using Bayesian analyses in OxCal, based on the Markov chain Monte-Carlo (MCMC) algorithm. We used standard codes and commands in OxCal, including P_Sequence, Sequence, and Phase. The Outlier code was also used because charcoal derives from vegetation that is, by definition, older than the fire that carbonized it.

Combine function

This description is adapted from Bunch et al. [11]. Two functions in OxCal are used for combining dates from a single inferred event. The 'R Combine' function is used to combine two or more radiocarbon dates from the same source, e.g., a single skeleton. The 'Combine' function tests two or more radiocarbon dates from different sources believed to be coeval, e.g., the date of the Hopewell burn layer. The 'Combine' routine is used here because there were burn layers representing radiocarbon from different sources at multiple sites. For the Combine function, a chi-squared test is automatically performed. An error message will be generated if the confidence limits drop below 5%, in which case, the dates cannot be considered coeval. The Hopewell sites passed the chi-squared test.

Synchronicity function

The description here and in the manuscript is from that study by Kennett et al. [82] using the protocol for testing synchroneity, as described in Bronk Ramsey [83], which is modified and presented here. We used OxCal's Sequence and Difference codes to determine the most likely common age interval for the 17 radiocarbon dates from the Hopewell burn layer. In this test, synchroneity is possible and is not rejected if the computed interval at 95% CI allows for a full overlap, i.e., includes zero years.

Acknowledgements

This article would not have been possible without the help of Steve Meyers, who unexpectedly passed away before the completion of the research. Even though he is deceased, Stephen Meyers is included as a co-author because he participated in collecting all the field data and writing the original manuscript. Field and laboratory work was undertaken between 2019 and 2021 as part of the University of Cincinnati-The Hopewell Comet Airburst Project, co-directed by Kenneth Barnett Tankersley and Stephen Meyers. Then, graduate students Louis Herzner and Dylan Zedaker assisted in the field and laboratory. James A. Jordan conducted the stable carbon isotope analyses, and Dr. David L. Lentz provided botanical analyses. We are especially grateful to Cory Christopher and the Cincinnati Nature Center, Mayor Mark Kobasuk and the Village of Newtown, the Greenlawn Cemetery of Milford, Steven Wetz and the City of Marietta, Ohio, Jessica Spencer, Adam McCosham and the Great Parks of Hamilton County, Paul Gardner and the Archaeological Conservancy, Jon Seymour and Oxbow Inc., Beth McCord and the Indiana State Historic Preservation Office of the Indiana Department of Natural Resources, Berea College, Ryan Merkle and the Scenic River Canoe Excursions, and Dale Eads of the Eads Earthwork site. We would like to thank Jenny Ruth Tankersley, Sarah C. Jantzi, and the Plasma Chemistry Laboratory at the Center for Applied Isotope Studies, University of Georgia, for their invaluable assistance. We greatly appreciate the volunteer efforts of Larry Sandman and the undergraduate student field assistance of Maria Nicole Saniel-Banrey, Harrison Todd Stanley, Benjamin Lewton, Sarah Jordan, and Maddie Moeller. The contributions of the journal editor and six anonymous reviewers were invaluable and significantly improved the manuscript. We are especially grateful to Drs. Allen West, Malcolm LeCompte, and Christopher Moore for helpful suggestions that improved the manuscript. Independent SEM and EDS analyses of the microspherules were conducted at the University of Utah, and independent SEM and EDS analyses of the micrometeorites were conducted at Elizabeth City State University.

Data availability

All the data generated or analyzed during this study are included in this published article and its Supplementary Information files).

Author contributions

K.B.T. conceived of the project and wrote most of the manuscript. K.B.T., S.D.M., and S.A.M. conducted the hand excavation, soil, and stratigraphic analyses. K.B.T. directed the laboratory work.

Funding

Field and laboratory work for this study was made possible with funding from the Charles Phelps Taft Foundation.

Competing interests

The authors declare no competing interests.

References

[1] Clube, V.; Napier, B. The Cosmic Serpent: A Catastrophist View of Earth History; Universe Books: New York, 1982.

[2] Burke, J.G. Cosmic Debris: Meteorites in History; University of California Press: Berkley, 1986.

[3] Firestone, R.B.; West, A.; Kennett, J.P.; Becker, L.; Bunch, T.E.; Revay, Z.S.; Schultz, P.H.; Belgya, T.; Kennett, D.J.; Erlandson, J.M.; et al. Evidence for an Extraterrestrial Impact 12,900 Years Ago that Contributed to the Megafaunal Extinctions and the Younger Dryas Cooling. *Proc. Natl. Acad. Sci.* **2007**, *104*(41), 16016–16021, doi:10.1073/pnas.0706977104.

[4] Moore, A.; Kennett, D. Cosmic Impact, the Younger Dryas, Abu Hureyra, and the Inception of Agriculture in Western Asia. *Eurasian Prehist.* **2013**, *10*(1–2), 57–66.

[5] Moore, A.M.T.; Kennett, J.P.; Napier, W.M.; Bunch, T.E.; Weaver, J.C.; LeCompte, M.A.; Adedeji, A.V.; Gunther Kletetschka, G.; Hermes, R.E.; Wittke, J,H.; et al. Abu Hureyra, Syria, Part 2: Additional Evidence Supporting the Catastrophic Destruction of this Prehistoric Village by a Cosmic Airburst ~12,800 years Ago. *ScienceOpen* **2023**, *1*(1), e20230003, doi:10.14293/ACI.2023.0002.

[6] Napier, W.M. In The Influx of Comets and their Debris. Accretion of Extraterrestrial Matter Throughout Earth's History; Peucker-Ehrenbrink, B., Schmitz, B., Eds.; Springer: Boston, MA, USA, 2001; pp. 51–74.

[7] Napier, W.M. Giant Comets and Mass Extinctions of Life. *Mon. Not. R. Astron. Soc.* **2015**, *448*(1), 27–36, doi:10.1093/mnras/stu2681.

[8] Napier, W.M. The Hazard from Fragmenting Comets. *Mon. Not. R. Astron. Soc.* **2019**, *488*(2), 1822–1827, doi:10.1093/mnras/stz1769.

[9] Rumpf, C.M.; Lewis, H.G.; Atkinson, P.M. Asteroid Impact Effects and their Immediate Hazards for Human Populations. *Geophys. Res. Lett.* **2017**, *44*, 3433–3440, doi:10.1002/2017GL073191.

[10] Pierazzo, E.; Garcia, R.R.; Kinnison, D.E.; Marsh, D.R.; Lee-Taylor, J.; Crutzen, P.J. Ozone Perturbation from Medium-Size Asteroid Impacts in the Ocean. *Earth Planet. Sci. Lett.* **2010**, *299*(3–4), 263–272, doi:10.1016/j.epsl.2010.08.036.

[11] Bunch, T.E.; LeCompte, M.A.; Adedeji, A.V.; Wittke, J.H.; Burleigh, T.D.; Hermes, R.E.; Mooney, C.; Batchelor, D.; Wolbach, W.S.; Kathan, J.; et al. A Tunguska Sized Airburst Destroyed Tall el-Hammam a Middle Bronze Age City in the Jordan Valley near the Dead Sea. *Sci. Rep.* **2021**, *11*(1), 1–64, doi:10.1038/s41598-021-97778-3.

[12] Tonry, J.L.; Denneau, L.; Heinze, A.N.; Stalder, B.; Smith, K.W.; Smartt, S.J.; Stubbs, C.W.; Weiland, H.J.; Rest, A. ATLAS: A High-Cadence All-Sky Survey System. *Publ. Astron. Soc. Pac.* **2018**, *130*, 064505, doi:10.48550/arXiv.1802.00879.

[13] Powel, J.L. Peer Review and the Pillar of Salt: A Case Study. *Res. Ethics* **2022**, *19*, 78–89, doi:10.1177/17470161221131491.

[14] Powel, J.L. Premature Rejection in Science: The Case of the Younger Dryas Impact Hypothesis. *Sci. Prog.* **2022**, *105*, 1–43, doi:10.1177/00368504211064272.
[15] Weitering, H. 'Tunguska'-Size Asteroid Makes Surprise Flyby of Earth. Space. April 16, 2018.
[16] Townsend, R.F.; Sharp, R.V. Hero, Hawk, and Open Hand: American Indian Art of the Ancient Midwest and South; Yale University Press: New Haven, 2004.
[17] Colavito, J. The Mound Builder Myth: Fake History and the Hunt for a "Lost White Race"; University of Oklahoma Press: Norman, 2020.
[18] Griffin, J.B. Eastern North American Archaeology: A Summary. *Science* **1967**, *156*, 175–191, doi:10.1126/science.156.3772.175.
[19] Willoughby, C.C.; Hooten E.A. Turner Group of Earthworks Hamilton County, Ohio, Papers of the Peabody Museum of American Archaeology and Ethnology; Harvard University: Cambridge, 1922.
[20] Wasson, J.T.; Sedwick S.P. Possible Sources of Meteoritic Material from Hopewell Indian Burial Mounds. *Nature* **1969**, *222*, 22–24, doi:10.1038/222022a0.
[21] Kalinowski, D.D. The Meteorites of Ohio; The Ohio State University: Columbus, 1972.
[22] Kimberlin, J.; Wasson, J.T. Comparison of Iron Meteoritic Material from Ohio and Illinois Hopewellian Burial Mounds. *Am. Antiq.* **1976**, *41*, 489–491, doi:10.2307/279015.
[23] Nolan, K.C.; Weiland, A.; Lepper, B.T.; Aultman, J.; Murphy, L.R.; Ruby, B.J.; Schwarz, K.; Davidson, M.; Wymer, D.; Everhart, T.D.; et al. Refuting the Sensational Claim of a Hopewell-Ending Cosmic Airburst. *Sci. Rep.* **2023**, *13*, 12910, doi:10.1038/s41598-023-39866-0.
[24] Bunch, T.E.; Hermes, R.E.; Moore, A.M.T.; Kennett, D.J.; Weaver, J.C.; Wittke, J.H.; DeCarli, P.S.; Bischoff, J.L.; Hillman, G.C.; Howard, G.A.; et al. Very High-Temperature Impact Melt Products as Evidence for Cosmic Airbursts and Impacts 12,900 Years Ago. *Proc. Natl. Acad. Sci.* **2012**, *109*(28), E1903–E1912, doi:10.1073/pnas.1204453109.
[25] Israde-Alcántara, I.; Bischoff, J.L.; Domínguez-Vázquez, G.; Li, H.-C.; DeCarli, P.S.; Bunch, T.E.; Wittke, J.H.; Weaver, J.C.; Firestone, R.B.; West, A.; et al. Evidence from Central Mexico Supporting the Younger Dryas Extraterrestrial Impact Hypothesis. *Proc. Natl. Acad. Sci.* **2012**, *109*(13), E738–E747, doi:10.1073/pnas.1110614109.
[26] LeCompte, M.A.; Goodyear, A.C.; Demitroff, M.N.; Batchelor, D.; Vogel, E.K.; Mooney, C.; Rock, B.N.; Seidel, A.W. Independent Evaluation of Conflicting Microspherule Results from Different Investigations of the Younger Dryas Impact Hypothesis. *Proc. Natl. Acad. Sci.* **2012**, *109*(44), E2960–2969, doi:10.1073/pnas.1208603109.
[27] Wittke, J.H.; Weaver, J.C.; Bunch, T.E.; Kennett, J.P.; Kennett, D.J.; Moore, A.M.T.; Hillman, G.C.; Tankersley, K.B.; Goodyear, A.C.; Moore, C.R.; et al. Evidence for Deposition of 10 Million Tonnes of Impact Spherules across Four Continents 12,800 y Ago. *Proc. Natl. Acad. Sci.* **2013**, *110*(23), E2088–E2097, doi:10.1073/pnas.1301760110.
[28] Wolbach, W.S.; Ballard, J.P.; Mayewski, P.A.; Adedeji, V.; Bunch, T.E.; Firestone, R.B.; French, T.A.; Howard, G.A.; Israde-Alcántara, I.; Johnson, J.R.; et al. Extraordinary Biomass-Burning Episode and Impact Winter Triggered by the Younger Dryas Cosmic Impact ~12,800 years Ago. 1. Ice Cores and Glaciers. *J. Geol.* **2018**, *126*(2), 165–184, doi:10.1086/695703.
[29] Wolbach, W.S.; Ballard, J.P.; Mayewski, P.A.; Parnell, A.C.; Cahill, N.; Adedeji, V.; Bunch, T.E.; Domínguez-Vázquez, G.; Erlandson, J.M.; Firestone, R.B.; et al. Extraordinary Biomass-Burning Episode and Impact Winter Triggered by the Younger Dryas Cosmic Impact ~12,800 years Ago. 2. Lake, Marine, and Terrestrial Sediments. *J. Geol.* **2018**, *126*(2), 185–205, doi:10.1086/695704.
[30] Pino, M.; Abarzúa, A.M.; Astorga, G.; Martel-Cea, A.; Cossio-Montecinos, N.; Navarro, R.X.; Lira, M.P.; Labarca, R.; LeCompte, M.A.; Adedeji, V.; et al. Sedimentary Record from Patagonia, Southern Chile Supports Cosmic-Impact Triggering of Biomass Burning, Climate Change, and Megafaunal Extinctions at 12.8 ka. *Sci. Rep.* 2019, 9(1), 4413, doi:10.1038/s41598-018-38089-y.
[31] Moore, C.R.; West, A.; LeCompte, M.A.; Brooks, M.J.; Daniel, I.R., Jr.; Goodyear, A.C.; Ferguson, T.A.; Ivester, A.H.; Feathers, J.K.; Kennett, J.P.; et al. Widespread Platinum Anomaly Documented at the Younger Dryas Onset in North American Sedimentary Sequences. *Sci. Rep.* **2017**, *7*, 44031, doi:10.1038/srep44031.
[32] Moore, C.R.; Brooks, M.J.; Goodyear, A.C.; Ferguson, T.A.; Perrotti, A.G.; Mitra, S.; Listecki, A.M.; King, B.C.; Mallinson, D.J.; Lane,C.S.; et al. Sediment cores from White Pond, South Carolina, contain a Platinum Anomaly, Pyrogenic Carbon Peak, and Coprophilous Spore Decline at 12.8 ka. *Sci. Rep.* **2019**, *9*(1), 1–11, doi:10.1038/s41598-019-51552-8.
[33] Moore, A.M.T.; Kennett, J.P.; Napier, W.M.; Bunch, T.E.; Weaver, J.C.; LeCompte, M.; Adedeji, A.V.; Hackley, P.; Kletetschka, G.; Hermes, R.E.; et al. Evidence of Cosmic Impact at Abu Hureyra, Syria at the Younger Dryas Onset (~12.8 ka): High-Temperature Melting at >2200 °C. *Sci. Rep.* **2020**, 4185, doi:10.1038/s41598-020-60867-w.
[34] Moore A.M.T.; Kennett J.P.; Napier W.M.; LeCompte M.A.; Moore C.R.; West A. Abu Hureyra, Syria, Part 3: Comet Airbursts Triggered Major Climate Change 12,800 years Ago that Initiated the Transition to Agriculture. *ScienceOpen* **2023**, *1*(1). doi:10.14293/ACI.2023.0004.
[35] Tankersley, K.B.; Meyers, S.A. The Eagle Station Impact Site. *North Am. Archaeol.* **2023**, *44*(2–3), 103–114, doi:10.1177/01976931231195111.
[36] Tankersley, K.B.; Meyers, S.A.; Stimpson, D.I.; Knepper, S.M. Evidence for a Large Late-Holocene Strewnfield in Kiowa County, Kansas, USA. *ScienceOpen* **2023**, *1*(1). doi:10.14293/ACI.2023.0005.
[37] Tankersley, K.B. Archaeological Geology of the Turner Site Complex, Hamilton County, Ohio. *North Am. Archaeol.* **2007**, *28*(4), 271–294, doi:10.2190/NA.28.4.a.
[38] Greber, N. Chronological Relationships Among Ohio Hopewell Sites: Few Dates and Much Complexity. In Theory, Method, and Practice in Modern Archaeology; Jeske, R.J., Charles, D.K., Eds.; Praeger Publishers: Westport, 2003; pp. 88–113.
[39] Shea, T.; Hammer, J.E.; Hellebrand, E.; Mourey, A.J.; Costa, F.; First, E.C.; Lynn, K.J.; Melnik, O. Phosphorus and Aluminum Zoning in Olivine: Contrasting Behavior of Two Nominally Incompatible Trace Elements. *Contrib. Mineral. Petrol.* **2019**, *174*, 85, doi:10.1007/s00410-019-1618-y.
[40] Schnetzler, C.C.; Walter, L.S.; Marsh, J.G. Source of the Australasian Tektite Strewnfield: A Possible Offshore Impact Site. *Geophys. Res. Lett.* **1988**, *15*(4), 357–360, doi:10.1029/GL015i004p00357.
[41] Hermes, R.E.; Wenk, H.-R.; Kennett, J.P.; Bunch, T.E.; Moore, C.R.; LeCompte, M.A.; Kletetschka, G.; Adedeji, A.V.; Langworthy, K.; Razink, J.J.; et al. Microstructures in Shocked Quartz: Linking Nuclear Airbursts and Meteorite Impacts. *ScienceOpen* **2023**, *1*(1). doi:10.14293/ACI.2023.0001.
[42] Ross, C.S. Optical Properties of Glass from Alamogordo, New Mexico. *Am. Mineral.* **1948**, *33*, 360–362.
[43] Blum, J.; Chamberlain, C.P.; Hingston, M.P.; Koeberl, C.; Marin, L.E.; Schuraytz, B.C.; Sharpton, V.L. Isotopic Comparison of K/T Boundary Impact Glass with Melt Rock from the Chicxulub and Manson Impact Structures. *Nature* **1993**, *364*, 325–327, doi:10.1038/364325a0.
[44] Gary Lofgren, G.; Lanier, A.B. Dynamic Crystallization Study of Barred Olivine Chondrules. *Geochim. Cosmochim. Acta* **1990**, *54*, 3537–3551, doi:10.1016/0016-7037(90)90303-3.
[45] Glass, B.P.; Burns, C.A. Microkrystites - A New Term for Impact-Produced Glassy Spherules Containing Primary Crystallites. *Proc. Lunar Planet. Sci. Conf.* **1988**, *18*, 455–458.
[46] Glass, B.P.; Simonson B.M. Distal impact ejecta layers: Spherules and more. *Elements* **2012**, *8*(1), 43–48, doi:10.2113/gselements.8.1.43.

[47] Glass, B.P.; Simonson B.M. Mesozoic Spherule/Impact Ejecta Layers. Springer, Distal Impact Ejecta Layers, 2013; pp. 245–320.
[48] Glass, B.P.; Simonson, B.M. Modeling Variations in Distal Impact Ejecta/Spherule Layers through Space and Time. *Distal Impact Ejecta Layers* **2013**, 533–594.
[49] Firestone, R.; West, A.; Warwick-Smith, S. The Cycle of Cosmic Catastrophes: How a Stone-Age Comet Changed the Course of World Culture; Bear and Company: Rochester, 2006.
[50] DePalma, R.A.; Smit, J.; Burnham, D.A.; Kuiper, K.; Manning, P.L.; Oleinik A.; Larson, P.; Maurrasse, F.J.; Vellekoop, J.; Richards, M.A.; et al. A seismically induced onshore surge deposit at the KPg boundary, North Dakota. *Proc. Natl. Acad. Sci. U. S. A.* **2019**, *116*, 8190–8199, doi:10.1073/pnas.1817407116.
[51] Tankersley, K.B.; Balantyne, M. X-ray Power Diffraction Analysis of Late Holocene Reservoir Sediments. *J. Archaeol. Sci.* **2010**, *37*, 133–138, doi:10.1016/j.jas.2009.09.023.
[52] Tankersley, K.B.; Meyers, S.A.; Albalushi, Jr., S.M.; Alhabsi, S.S.S.; Bowers, P.S.; Burton, I.L.; Loukinas, A.C.M.; Ward, S.L.; Chaney, S. The Eads Earthwork: Implications for Hopewell Ceremonialism. *North Am. Archaeol.* **2023**, *44*(1), 43–58, doi:10.1177/01976931221128608.
[53] Tankersley, K.B.; Lyle, N. Holocene Faunal Procurement and Species Response to Climate Change in the Ohio River Valley. *North Am. Archaeol.* **2019**, *40*(4), 192–235, doi:10.1177/0197693119889256.
[54] Tankersley, K.B.; Dunning, N.P.; Owen, L.A.; Huff, W.D.; Park, J.H.; Kim, C.; Lentz, D.L.; Sparks-Stokes, D. Positive Platinum anomalies at three late Holocene high magnitude volcanic events in Western Hemisphere sediments. *Sci. Rep.* **2018**, *8*, 11298, doi:10.1038/s41598-018-29741-8.
[55] Tankersley, K.B.; Murari, M.K.; Crowley, B.E.; Owen, L.A.; Storrs, G.W.; Mortensen, L. Quaternary Chronostratigraphy and Stable Isotope Paleoecology of Big Bone Lick, Kentucky, USA. *Quatern. Res.* **2015**, *83*, 479–487, doi:10.1016/j.yqres.2015.01.009.
[56] Tankersley, K.B.; Wells, D. Further Evaluation of Fluoride Dating by Ion Selective Electrode. *North Am. Archaeol.* **2011**, *32*(3), 249–268, doi:10.2190/NA.32.3.b.
[57] Simonson, B.M.; Glass B.P. Spherule Layers—Records of Ancient Impacts. *Annu. Rev. Earth Planet. Sci.* **2004**, *32*, 329–361, doi:10.1146/annurev.earth.32.101802.120458.
[58] Brose, D.S.; Greber, N. Hopewell Archaeology: The Chillicothe Conference; Kent State University Press, Kent, 1979.
[59] Byers, A.M.; Wymer, D.A. Hopewell Settlement Patterns, Subsistence, and Symbolic Landscapes; University of Florida, Gainsville, 2010.
[60] Fagan, B. Ancient North America; Thames & Hudson: London, 2005.
[61] Atwater, C. Descriptions of the Antiquities Discovered in the State of Ohio and Other Western States; Transactions and Collections of the American Antiquarian Society: Worcester, 1820.
[62] Squier, E.; Davis, E. Ancient Monuments of the Mississippi Valley; Smithsonian Institution: Washington DC, 1848.
[63] Prufer, O. The Hopewell Complex of Ohio. In Hopewellian Studies; Caldwell, J.; Hall, R., Eds.; Illinois State Museum: Springfield, 1964; pp. 37–83.
[64] Prufer, O. Ohio Hopewell Ceramics, An Analysis of the Extant Collections; University of Michigan: Ann Arbor, 1968.
[65] Coon, M.S. The Oberting Site (12d25): An Ohio Hopewell Enclosure in Indiana; Purdue University: West Lafayette, 2008.
[66] Riordan, R.V. The Enclosed Hilltops of Southern Ohio. In A View from the Core: A Synthesis of Ohio Hopewell Archaeology; Pacheco, P.J., Ed.; Ohio Archaeological Council: Columbus, 1996; pp. 242–256.
[67] Riordan, R.V. Boundaries, Resistance, and Control: Enclosing the Hilltops in Middle Woodland Ohio. In Ancient Earthen Enclosures of the Eastern Woodlands; Mainfort, R.; Sullivan, L., Eds.; University of Florida Press: Gainesville, 1998; pp. 68–84.
[68] Romain, W.F. Hopewellian Geometry; Forms at the Interface of Time and Eternity. In A View from the Core: A Synthesis of Ohio Hopewell Archaeology; Pacheco, P.J., Ed.; Ohio Archaeological Council: Columbus, 1996; pp. 194–209.
[69] Deloria, V. Red Earth White Lies: Native Americans and the Myth of Scientific Fact; Scribner Press: New York, 1995.
[70] Cajete, G. Native Science: Natural Laws of Interdependence; Clear Light Press: Santa Fe, 1992.
[71] Angulo, J. Teotihuacan: Aspectos de la Cultura a través de su Expresión Pictórica. In La Pintura Mural Prehispánica en México; de Lafuente, B., Ed.; Universidad Nacional Autónoma de México, 2018; pp. 65–186.
[72] Tankersley, K.B.; Meyers, S.D.; Meyers, S.A.; Lentz, D.L. Reply to: Arguments for a Comet as Cause of the Hopewell Airburst are unsubstantiated. *Sci. Rep.* **2022**, *12*, 12113, doi:10.1038/s41598-022-16212-4.
[73] Emel'yanenko, V.V.; Popova, O.P.; Chugai, N.N.; Shelyakov, M.A.; Pakhomov, Y.V.; Shustov, B.M.; Shuvalov, V.V.; Biryukov, E.E.; Rybnov, Y.S.; Marov, M.Y.; et al. Astronomical and Physical Aspects of the Chelyabinsk Event. *Sol. Syst. Res.* **2013**, *47*, 240–254, doi:10.1134/S0038094613040114.
[74] Jenniskens, P.; Popova, O.P.; Glazachev, D.O.; Podobnaya, E.D.; Kartashova, A.P. Tunguska Eyewitness Accounts, Injuries, and Casualties. *Icarus* **2019**, *327*, 4–18, doi:10.1016/j.icarus.2019.01.001.
[75] Krinov, E.L. Giant Meteorites; Pergamon Press: Oxford, 1966.
[76] McCoy, T. Ašiihkiwi neehi kiišikwi myaamionki: Earth and Sky: The Place of the Myaamiaki; Miami Tribe of Oklahoma: Miami, 2011.
[77] Morgan, L.H. League of the Ho-dé-no-sau-nee or Iroquois; Sage Publishing: Rochester, 1851.
[78] Spencer, J. Shawnee Folk-Lore. *J. Am. Folk.* **1909**, *22*, 319–326, doi:10.2307/534746.
[79] Howard, J.H. Shawnee: The Ceremonialism of a Native Indian Tribe and Its Cultural Background; Ohio University Press: Columbus, 1981.
[80] Ruddell, S. Reminiscences of Tecumseh's Youth; Wisconsin Historical Society: Madison, 2003.
[81] Smith, K.B. Tunguska Revisited: 111-Year-Old Mystery Impact Inspires New, More Optimistic Asteroid Predictions; NASA6, 2019, p. 27.
[82] Kennett, J.P.; Kennett, D.J.; Culleton, B.J.; Aura Tortosa, J.E.; Bischoff, J.L.; Bunch, T.E.; Daniel, I.R., Jr.; Erlandson, J.M.; Ferraro, D.; Firestone, R.B.; et al. Bayesian Chronological Analyses Consistent with Synchronous Age of 12,835–12,735 Cal B.P. for Younger Dryas Boundary on Four Continents. *Proc. Natl. Acad. Sci. U. S.A.* **2015**, *112*, E4344–4353, doi:10.1073/pnas.1507146112.
[83] Ramsey, C.B. Bayesian Analysis of Radiocarbon Dates. *Radiocarbon* **2009**, *51*, 337–360, doi:10.1017/S0033822200033865.
[84] https://zenodo.org/records/10511513 (10.5281/zenodo.10511513).